NOAA/NWS METEOROLOGICAL ASSESSMENT FOR TYPHOON PONGSONA IN: POHNPEI STATE, FSM; CHUUK STATE, FSM; GUAM; AND, ROTA, CNMI

By

The National Oceanic and Atmospheric Administration (NOAA) National Weather Service (NWS) Meteorological Assessment Team for Typhoon Pongsona

Charles 'Chip' Guard, NWS Forecast Office Guam
Arthur N. L. Chiu, University of Hawaii at Manoa
Mark A. Lander, University of Guam

April 2003

1. Background: On 2 December 2002, a disturbance began to organize near 6.5N 165E, or about 370 miles east of Pohnpei. This late season disturbance was associated with an El Niño-induced westerly wind burst that would produce Pongsona and a twin disturbance in the Southern Hemisphere that later became Cyclone Yolande (04P). This type of tropical cyclone development has been described in various ways by Lander (1990, 1994); Dickenson and Molinari (2002). At 1100 UTC on 2 December, the Joint Typhoon Warning Center (JTWC) issued a Tropical Cyclone Formation Alert indicating that the circulation associated with the disturbance was likely to become a significant tropical cyclone in the subsequent 12 to 24 hours. Seven hours later, JTWC issued the first warning on Tropical Depression (TD) 31W, located at that time near 7.4N 163.5E. At 0000 UTC on 3 December, the JTWC upgraded the Depression to Tropical Storm (TS) 31W as it continued on a northwest track. TS 31W was named Tropical Storm Pongsona (pronounced Bong-sahn-WAH or Pong-sahn-WAH) by RSMC-Tokyo at 1200 UTC on 3 December, as it took a more westward track. Figure 1 shows Pongsona as it was developing on 3 December with 35-40 knot (39-44 mph) sustained winds.

TS Pongsona passed about 70 n mi (81 miles) south of Ujelang in the western Marshall Islands on 3 December at 2100 UTC, and then began to move to the west-southwest in the direction of Pohnpei State. After nearly 24 hours of this motion, Pongsona took a more westward track and passed some 60 n mi (69 miles) to the north of Pohnpei Island with 55-knot (63-mph) winds. At 0600 UTC on 5 December, Pongsona was upgraded by JTWC to typhoon status, and a few hours later, it passed to the north of Oroluk Atoll in northern Pohnpei State. From 0300 UTC to 0900 UTC on 6 December, Pongsona, packing 75- to 80-knot (86- to 92-mph) winds, moved just north of the Hall Islands in northern Chuuk State. After pounding and submerging parts of the small islets, the typhoon headed toward the Mariana Islands.

In response to the close agreement of nearly all tropical cyclone computer forecast models, Pongsona was predicted by JTWC to take a northward turn and pass east of Guam, toward Saipan and Tinian, with only slow intensification. On the early morning of 8 December, the typhoon came into the range of the Andersen Air Force Base (AFB) Weather Surveillance Radar—1988 Doppler (WSR-88D), which indicated that the typhoon was continuing to move on a more west-northwest track toward Rota and Guam. While Pongsona did eventually turn to the north, the northward turn was delayed some 24 hours, taking it west of Saipan and Tinian, but much closer to Guam and Rota. The center of the eye passed to within 10 n mi (12 miles) of Guam's northeast coastline, with the southwestern semicircle of the eye wall cloud traversing most of the island. In the 18-hour period from 1800 UTC 7 December until its peak intensity at 1200 UTC 8 December, Pongsona intensified from 105 knots (121 mph) to 130 knots (150 mph), reaching the super typhoon status of 130 knots (150 mph) while the center of the eye was northwest of Guam and the southeastern eye wall cloud was just off of the northwestern part of the island.

After passing over Guam, Pongsona continued on a northwest track, where it also pummeled Rota, especially the southwestern part of the island. After passing west of Rota, the intense typhoon moved to the north, west of Tinian and Saipan. On 9 December, it recurved to the northeast near 18N 144E, and on 11 December, it became extratropical. Figure 2 shows the track of Typhoon Pongsona: during its development; during the period it affected Chuuk State, Pohnpei State, Guam, and Rota, Tinian, Saipan, and the northern islands of the Commonwealth of the Northern Mariana Islands (CNMI); and, during its recurvature and extratropical transition. Ujelang in the western Marshall Islands was affected early in the storm's life but is not inhabited.

The following sections summarize the meteorological and hydrological aspects of Pongsona's passage through Micronesia. For Guam and Rota, the information is used to make a determination of the most likely intensity of Typhoon Pongsona as it traversed the islands. This analysis is in support of the NWS-directed assessment of the winds over Guam and Rota for Pongsona.

2. Pohnpei State

a. Track: A visible eye had not yet developed as Typhoon Pongsona approached Oroluk Atoll in Pohnpei State early on 6 December. The cyclone center passed Oroluk at around 0000 UTC on 6 December. This path is based on a combination of surface wind and pressure observations from the Automatic Meteorological Observing Station (AMOS) weather instrument on Oroluk (WMO98345) and from satellite imagery (e.g. Figure 3).

b. Wind: Pongsona did not affect Pohnpei Island much, where a peak wind of only 39 knots (45 mph) was observed at 1058 UTC on 5 December. At the Oroluk AMOS, the highest sustained wind was from 210º at 31 knots (36 mph) at 0100 UTC on

6 December. This occurred just after the center passed the island to the east. The highest gust measured was from 230º at 54 knots (62 mph) at 1300 UTC on 5 December.

c. Pressure: The minimum sea level pressure at Pohnpei was 999.8 hPa at 0258 UTC and at 0354 UTC on 5 December. The minimum sea level pressure at Oroluk was 990.8 hPa at 1100 UTC on 5 December.

d. Rainfall: Rainfall at Oroluk was not measured as the sensor on the AMOS was inoperative. Twenty-four-hour rainfall at Pohnpei was 2.24 inches from 0600 UTC 4 December 2002 to 0600 UTC 5 December 2002. The greatest 6-hour rainfall was 0.63 inches ending at 1800 UTC 4 December.

e. Storm Surge: Storm surge and inundation were not observed on Pohnpei. There may have been some inundation of taro patches and other low-lying coastal areas on Oroluk from high waves and surf.

f. Flooding and Mudslides: There were no reports of flooding or mudslides on Pohnpei.

g. Damage Assessment: To our knowledge, no formal damage assessment was conducted and damage was minimal.

3. Chuuk State

a. Track: A visible eye had not yet developed as Pongsona moved north of Chuuk Lagoon. The cyclone center passed 90 n mi (104 miles) north of Weno Island, Chuuk Lagoon, Chuuk State at around 0600 UTC on 6 December. This path is based on a combination of surface wind and pressure observations from the Weather Service Office (WSO) at Chuuk, from the AMOS at Ulul Island (WMO91328) in Namonuito Atoll, and from satellite imagery (Figure 3). Observations and reports from Fananu and Murilo Atolls in the Hall Islands suggest that the typhoon passed very close to these islands with typhoon force winds. Seawater covered much of the islands.

b. Wind: The maximum sustained wind observed at WSO Chuuk was from 290º at 43 knots (49 mph) at 0859 UTC with maximum gusts from 240º at 59 knots (68 mph) at 0936 UTC on 6 December. The AMOS at Ulul in Namanuito Atoll (WMO98325), about 175 n mi (201 miles) west-southwest of the typhoon, indicated a sustained wind from 310º at 30 knots (35 mph) at 1201 UTC and a peak gust from 310º at 48 knots (55 mph) at 1201 UTC and 1301 UTC. At Satawan Atoll (WMO91338), 210 n mi (242 miles) south of the typhoon, the maximum observed sustained wind measured by the AMOS was from 210º at 31 knots (36 mph) at both 1201 UTC and 1301 UTC. The peak observed gust was 51 knots (58 mph) from 310 degrees at 2001 UTC on 5 December.

c. Pressure: The minimum pressure at WSO Chuuk was 993.2 hPa at 0553 UTC on

6 December. The pressure at Ulul was 992.8 hPa at 1301 UTC on 6 December. At Satawan, the minimum pressure was 999.5 hPa at 0401 UTC on 6 December.

d. Rainfall: Rainfall reported at the Weather Service Office at Weno Island, Chuuk is shown in Table 1.

Table 1. Rainfall amounts in inches at WSO Chuuk for 1-hour, 6-hour, 12-hour, and 24-hour periods on 5 and 6 December.

Period (hour)	Amount (inches)	Date/Time ending at (UTC)
1	1.37	06/0100
6	3.29	06/0200
12	5.05	06/0800
24	7.13	06/0900

e. Storm Surge: Eye witness reports at Fananu Island and Nomwin Island in the Hall Islands indicated "high tides washing up over lands". "Taro patches and the low-lying parts of the islands, especially the coastal areas, are covered under water." With reference to beach erosion, "especially the Hall Islands, including Fananu and Nomwin, have their beaches wash out from inland due to high tides and coastal waves". At Weno Island in Chuuk Lagoon, "parts of the roads on Weno, especially the boat pool area and Mechitiw, are eroded from high tides washing up on lands".

f. Flooding and Mudslides: There were not reports of mudslides on the high islands of Chuuk Lagoon. There was some flooding on Weno Island as indicated from the statement: "The same low-lying areas near the airport are again submerged under water due to runoffs from the higher areas and the heavy rainfall."

g. Damage Assessment and other storm effects: The weather station at Weno, Chuuk reported "minor injuries from fallen coconut trees and broken glasses in the Hall Islands of Fananu and Ruo". In addition, "taro patches on Fananu inundated by saltwater, reported total destruction of houses…also animals, such as hogs, dogs, [and] chickens raised for food, totally wiped out". Overall, "the Hall Islands, including Murilo, Ruo, Fananu, and Nomwin, were mostly devastated by Typhoon Pongsona, as it passed just to the north of them."

4. Guam

a. Methodology for wind assessment on Guam and Rota

1). Techniques:

Because direct wind measurement systems either failed or did not provide adequate coverage, the assessment of the maximum winds over Guam and Rota required an in-

depth look at varying types of data. These data included: available sustained wind and wind gust measurements; sea level pressure measurements; storm surge/inundation measurements including run-up and still water levels; rainfall measurements; available weather radar and meteorological satellite data; and, the damage to structures, infrastructure and vegetation. By meshing observations and theory, it is possible to progressively whittle down the likely maximum winds to a narrow range, and to propose a single value as the most likely maximum 1-minute average, 10-meter height wind speed as the typhoon traversed Guam and Rota. Subsequently in this assessment, the terms intensity and maximum 1-minute average, 10-meter height sustained wind will be used interchangeably. Most Guam locations discussed in this assessment are shown in Figure 4.

a). Winds: The techniques used to evaluate the wind observations are those described in: Powell and Houston (1996a, b); Houston, Forbes, and Chiu (1999, 2002); and, Guard and Lander (1999). Techniques of Fujita (1971, 1992) were used to assess anomalous hurricane transients and tornados, and to determine *first wind* and *second wind* contributions. Because of the differing gust factors over land and water, the maximum sustained wind over land will be referred to as the over-water equivalent (OWE) value. This OWE is associated with a discrete gust as provided in warnings by the Joint Typhoon Warning Center. All winds are converted to 1-minute average, 10-meter elevation. Two-minute winds were converted to 1-minute winds using a conversion factor from Krayer and Marshall (1992): $w_{1min}=1.08\ w_{2min}$. Conversion to 10-meter height (when necessary) was accomplished using a logarithmic wind profile (Holton 1992). Knots were converted to miles-per-hour (mph) using the factor: $w_{mph}=1.15\ w_{kts}$.

b). Pressure: Sea level pressure data were the most complete data set available over Guam. The minimum observed sea level pressure over Andersen Air Force Base was very close to the minimum pressure in Pongsona at that time. Various wind-pressure relationships (e.g., Atkinson and Holliday (1975), Kraft (1961), Callaghan and Smith, 1998)) were considered. The rationale for choosing a specific wind-pressure relationship is shown in Figure 5. The intensity can also be estimated by applying the observed pressure gradient, and eye and eye wall cloud characteristics to a parametric wind model based on a tropical cyclone wind-pressure profile (e.g., Holland (1980)). The observed minimum sea level pressure in the eye can also be used in concert with satellite data to assess potential wind-pressure relationships.

c). Storm surge data: Storm surge refers to the height of the inundation in reference to mean sea level. The storm surge measurements associated with Pongsona can be compared with storm surge measurements of past cyclones affecting a location. In the case of Pongsona, the Typhoon Paka storm surge data were very useful. Considerable historical data describing the effects of the coral reefs on the actual coastal inundation are available for Guam (JTWC (1991); Guard et al. (1999)). Guard and Lander (1999), but these data are not available for Rota. Lander and Guard (1999) present coastal wave-cyclone intensity relationships for Guam derived from historical typhoon data and parametric wave model computations for typhoons of various size, intensity, and location.

d). Doppler weather radar data: While the AAFB WSR-88D lost power just before the eye entered Guam, the western eye wall cloud was already over the island. Some characteristics of the eye wall cloud could be evaluated, including the inbound and outbound wind components. The maximum winds observed near Guam were within a few hundred feet of the surface due to the nearness of the eye wall cloud to the radar.

e). Meteorological satellite data: Tropical cyclone intensity can be determined from visible and infrared meteorological satellite data using the techniques of Dvorak (1975, 1984). The techniques are universally used in all tropical cyclone-prone basins in the world. The Dvorak technique can be applied both manually and automatically. The manual technique has routinely been used operationally. The automated techniques, however, provide an objective "sanity check" for both the absolute value and the trend, and have been gaining popularity as a result of recent improvements (Velden et al. 1998). The Japanese Geostationary Meteorological Satellite (GMS-5) provides hourly data, which enables hourly analyses. These satellite data are complete for the entire life of the cyclone. Additional satellite data include microwave imagery from the Tropical Rainfall Measuring Mission (TRMM) and Defense Meteorological Satellite Program (DMSP) satellites, and ocean surface wind speed estimates from the SeaWinds scatterometer.

f). Rainfall data: There is a fairly dense rain gauge network on Guam. However, there are failures in the network during typhoons. The amount and distribution of rainfall on Guam and their relationships to the eye wall cloud location can provide some general information about the cyclone intensity. While there is a general relationship between the rainfall rate in the eye wall cloud and the typhoon's intensity, it is very difficult to accurately integrate the amounts for the total storm. Thus, in practice, these data are the least useful for maximum wind estimation. However, the patterns of the heaviest rains and the highest winds in the eye wall cloud should match fairly closely. A simple rainfall distribution model (Figure 6) is used to smooth the actual rainfall values and derive a more representative rainfall distribution. This distribution model assumes that a similar rainfall gradient exists across the eye wall cloud and that the annulus is relatively uniform. Thus, areas that remain in the eye wall cloud will get more rain than those that actually experience eye passage, since no rain is falling in the eye.

g). Damage assessment: An assessment of the wind-induced damage to structures, infrastructure, and vegetation can provide extremely valuable insight about the maximum winds in tropical cyclones. The Saffir-Simpson Hurricane Scale (Saffir 1972), Simpson (1974) and the Saffir-Simpson Tropical Cyclone Scale (Guard and Lander 1999) have been used in the coastal US and in the western North Pacific tropics, respectively. These scales divide hurricanes/typhoons into five graduated wind categories that relate the wind to the levels of damage, with Category 1 being the least severe and Category 5 being the most severe. The damage increases rather exponentially with the wind speed. While there are only five damage Categories, these can be sub-divided into low, medium, and high sub-divisions. While the duration of the winds can affect the total damage within a wind-damage category and increase the sub-division, it does not generally cause an

increase in the Category number. Techniques used in the damage assessment are those used in many other severe storm assessments (e.g., FEMA (1993), Houston et al. (1999), Marshall (2002)). Additional tropical cyclone information and typhoon vulnerability information about Guam are extracted from Guard et al (1999).

2). Considerations in making the assessments on Guam:

The goal in determining the maximum intensity of Pongsona while it was over Guam and near Rota is to determine the cyclone's maximum intensity over water and the smoothed wind distribution over the islands. Both Guam and Rota are rugged high islands with terrain, vegetation, and man-made objects that can modify these winds, and that can greatly affect exposure to the wind. The modifications can act to make the winds higher or lower than over water. The over-water determination for the typhoon's maximum intensity is established by convention, and allows for a standardized method for comparing one typhoon with another. The number of high-rise buildings, the variety of structures, and the density of structures make the determination of the winds over Guam much more complex than the determination of the winds over Rota. In addition, the residual effects of Typhoon Chata'an, which made a direct hit on Guam with maximum sustained winds of 90 knots (104 mph) in July 2002, must be considered in the assessment.

a). The maximum intensity is that wind over water. Winds may be somewhat stronger or weaker over land, as a result of terrain (mountains, valleys, cliffs, bluffs, etc.), surface roughness (trees, brush, grass, sand, etc.), and man-made objects (buildings, storage tanks, towers, etc.). The terrain, surface roughness, and man-made objects can increase or decrease the wind, and can greatly affect the exposure to the winds. Thus, the peak gust is a more realistic measurement of the wind over land, and the 3-second peak gust is now the design standard recommended by the American Society of Civil Engineers (ASCE).

b). The amount of debris will be less than expected, since Typhoon Chata'an blew down much of what 100 mph winds would blow down. This debris was picked up in July, August, and September. On the other hand, Chata'an likely weakened some stronger structures, making them more vulnerable to Pongsona's winds.

c). The maximum winds hit in the daytime. The wind intensity is generally perceived as higher by the populace when seen in daylight hours than merely when heard at night.

d). Many witnesses perceive that the latest intense typhoon was the most severe of the historical typhoons. Recent memory in such events is more vivid than past memory. Even if past recollections are accurate, the person's location with respect to the maximum wind needs to be known. The wind direction at the time of the peak wind can vary considerably from typhoon to typhoon, and can affect the actual distribution of the wind speed and the perception of the wind speed.

b. Track and eye passage: While over Guam, the eye of Pongsona extended from central Guam to near the island of Rota (Figure 2). The western half of the eye entered the northeast side of Guam at about 0600 UTC on 8 December and exited the northwest side of the island about 0830 UTC the same day. The relative calm of the eye lasted about 2 hours and 30 minutes at Andersen Air Force Base to only a few minutes in parts of southwestern Dededo and northeastern Mangilao (Figure 7). Most of the southern half of the island remained in the eye wall cloud, being pounded continuously by strong winds and heavy rains. The center of the eye was approximately 8 n mi (9 miles) east-northeast of Andersen Air Force Base at the time of its closest point of approach to Guam, and approximately 50 n mi (58 miles) north of Guam and about 25 n mi (29 miles) west-northwest of Rota when it became a super typhoon. Table 2 lists the estimated time of eye duration at various locations on Guam, most of which were determined from interviews of island residents.

Table 2. Eye passage times as determined from interviews at various locations on Guam and from recording rain gauge values at Andersen Air Force Base.

Andersen AFB	1600L to 1830L	0600 UTC to 0830 UTC
South Finagayan (Dededo)	1645L to 1815L	0645 UTC to 0815 UTC
Perez Acres (Yigo)	1630L to 1800L	0630 UTC to 0800 UTC
Macheche (Dededo)	1645L to 1730L	0645 UTC to 0730 UTC
Latte Heights (Dededo)	1630L to 1715L	0630 UTC to 0715 UTC
Pagat (Mangilao)	1615L to 1630L	0615 UTC to 0630 UTC

c. Wind: Virtually all of the wind sensors on the island either failed physically or due to communications loss, or, in the case of the HANDARs, which use a Vaisala 425A three pronged ultrasonic wind sensor, provided erroneous data during the period of maximum winds. Appendix A lists the maximum wind observations over Guam, their locations, the type of wind sensor used, the elevation of the sensor, and the wind averaging time of the sensor. The maximum 2-minute sustained wind at Tiyan Guam was 270º at 92 knots (106 mph) at 0826 UTC on 8 December (observed by tower personnel using a non-recording F420 cup anemometer). This occurred during the second wind when tower personnel returned to temporarily observe the winds. The peak gust observed by the Automated Surface Observing System (ASOS) was 102 knots (117 mph) from 350º at 0508 UTC. This occurred during the first wind, just before the transmitter blew down. The peak wind may have occurred at sometime between these two observations. (The ASOS receiver was located on a Rohn tower that was blown down during the typhoon. The receiver was re-sited once winds fell to a safe speed.) The anemometer at Andersen Air Force Base failed at a very low wind speed (69 knots/79 mph) due to unknown reasons. However, the Andersen weather observers estimated a peak wind from 350º at 100 knots (115 mph) with gusts to 130 knots (150 mph) at 0459 UTC. On the west side of the island, the NOAA Ocean Service (NOS) tidal station at the inner Apra Harbor recorded a sustained wind of 83 knots (95 mph) from 359º at 0700 UTC and a peak gust of 101.3 knots (117 mph) from 354º at 0800

UTC. A Navy Davis Easymount Weather Monitor 2 system, also at the inner Apra Harbor, recorded a 1-minute sustained wind of 69.6 knots (80 mph) with a peak gust of 110.4 knots (127 mph) at 080530 UTC. The instrument failed at 080630 UTC. The HANDAR at outer Apra Harbor recorded a peak wind gust of 63.9 knots (73 mph) at 0100 UTC just before it began to give erroneous data. At Merizo, on the south end of the island, the peak gust recorded was 54 knots (62 mph) at 0252 UTC before it began to give erroneous data. The data from the Mangilao (east-central side of the island) HANDAR gave a peak gust of 56 knots (64 mph) before it sent out erroneous data. Finally, the Inarajan-Dan Dan (southeast side of Guam) HANDAR provided a reliable gust to 66 knots (76 mph) before it began transmitting erroneous data. In every case, the four HANDAR units produced no usable data during the several hours of strongest wind and heavy rains. Another Davis private weather station in Sinajana recorded a peak gust of 127 mph (110 knots) at 0550 UTC (first wind) and another later gust of 112 mph (97 knots) at 0817 UTC (second wind). It should be noted that this anemometer has poor exposure to the west because of a large tree, and that this likely reduced the speed of the second wind. Despite the failures of most of the gauges, the available wind data and the wind patterns support a typhoon with wind intensities greater than 100 knots (115 mph) with gusts greater than 125 knots (144 mph). Appendix A lists the locations of the anemometers, the type of wind-measuring equipment used, the sensor elevation, the wind averaging period, and the time and value of the maximum sustained wind and the peak gust.

The 92-knot (106-mph) 2-minute sustained wind recorded by Air Traffic Control (ATC) personnel at the Guam International Airport tower at 0826 UTC is a candidate observation for a potential maximum wind in Pongsona. Eye witness reports from Upper Tumon Bay (e.g., a security camera video at a shop near the Outrigger Hotel indicating that the interior glass doors blew in at exactly 0820 UTC), and the wind measurement at Sinajaña indicating a maximum west wind event at approximately 0820 UTC, suggest that this was the timing of peak wind across much of central Guam. Thus, the tower measurement deserves further scrutiny and emphasis. The wind instrument providing data to the ATC tower is located on the southwestern side of the airfield between the two main runways oriented 060-240. The anemometer is at a height of approximately 6 meters. Using a log-wind profile for a well-exposed, flat, open area allows one to estimate the 10-meter value as 108% of the 6-meter value (this is assuming a z_0 of 0.01 m) (Holton 1992). Thus, the 92 knots at 6 meters can be adjusted upward to an estimated 99 knots (114 mph) at 10 meters. A further conversion is made to estimate the 1-minute sustained wind speed value. Using ratios that appear in Krayer and Marshall (1992), the 1-minute sustained wind is approximately 108% of the 2-minute sustained wind. This allows a final estimate of the tower wind of 107 knots (123 mph) 1-minute sustained at 10-meter height. Using an exposure C (open field) gust factor of 1.3, a peak gust of 139 knots (160 mph) can be associated with the 107-knot 1-minute sustained wind.

d. Pressure: Minimum sea-level pressure within the eye of Pongsona was 937.1 hPa at 0900 UTC at Andersen AFB. If this value is used as the minimum SLP, it would correspond to 105 knots (121 mph) sustained winds based on the Atkinson-Holliday wind-pressure relationship commonly used in the Pacific basin. However, late season

typhoons in this region often better fit the wind-pressure relationship used in the Atlantic. The Atlantic scale (Kraft 1961) gives a maximum sustained wind of about 122 knots (141 mph) for a pressure of 937.1 hPa. Figure 5 illustrates the wind-pressure relationship used for Typhoon Pongsona. While the actual center of the eye was approximately 8-10 n mi (9-12 miles) northeast of Andersen Air Force Base, the lowest sea level pressure at the center was not likely lower than 935 hPa, which would correspond to about 107 knots (123 mph) using the Atkinson and Holiday wind-pressure scale, and 124 knots (143 mph) using the Atlantic relationship. In comparison, Paka's minimum pressure was also estimated to be 935 hPa when it passed Guam, and its intensity was estimated at 125 knots (144 mph). Other pressures observed on the island during Pongsona, while not in the eye, provide information useful for estimating the maximum wind from the pressure gradient.

The pressure difference between the NOS tidal gauge at Apra Harbor (959.8 hPa) and the International Airport (940.8 hPa) was 19.0 hPa, and the distance between the two was 7.3 n mi (8.4 miles). This is an average gradient of 2.6 hPa/n mi (2.3 hPa/mile). At a radius of 22.1 n mi (25.6 miles) from the center of Pongsona, this pressure gradient yields a gradient wind of approximately 140 knots (162 mph). The gradient wind typically provides a good estimate of the gust envelope of tropical cyclone surface winds. The 1-minute sustained over-water wind associated with this gust is 115 kt (133 mph). Since average values were used, this wind speed should be considered a lower bound for Pongsona's intensity as it passed over Guam.

e. Rainfall: Rainfall from Typhoon Pongsona was heavy across central parts of the island, with some locations receiving nearly 20 inches. The 24-hour rainfall for WFO Guam was 19.67 inches ending at 081350 UTC. A NASA TRMM tipping-bucket recording rain gauge at the University of Guam in Mangilao measured a 24-hour rainfall total of 25.61 inches and a maximum 1-hour rain rate of 6.58 inches. Preliminary data from USGS recording rain gauges on Guam provided an estimated 24-hour total of 15.84 inches at Mt. Chachao near Nimitz Hill. Maximum 1-hourly rain rates were 4.92 inches at Mt. Chachao, 4.20 inches at the Fena Reservoir, and 4.08 inches at Windward Hills. Data from these stations indicated hourly rainfall rates as high as 4.9 inches in one hour, 11.2 inches in 3 hours, 13.6 inches in 6 hours, and 16.08 inches in 24 hours. While these rainfall values from the USGS gauges are not as heavy as those observed in Typhoon Chata'an on 5 July 2002 (estimated at a 100-year rainfall event), they are large values and may exceed a 50-year rainfall event. The swath of heaviest rainfall in Pongsona was north of that during Chata'an. USGS stream gauges showed record levels of stream flow and stage height at the Asan River (peak stage 13.75 feet) near Asan on the western coast of central Guam and at the Pago River (peak stage 23.85 feet) near Ordot in east central Guam. Other Guam rivers to the south had very high peak stages as well, but these were not as high as the record levels during the Chata'an event. Rainfall amounts at various stations around Guam are listed below in Table 3. An analysis of the 24-hour rainfall, which is close to the storm total rainfall, is shown in Figure 8.

Table 3. Rainfall rates in inches from several different Guam sites. USGS measurements are preliminary and are shown as approximations. Ending times are in UTC.

Location	1-hr (ending at)	3-hr (ending at)	6-hr (ending at)	24-hr (ending at)
WFO Guam				19.67 (082354)
Andersen AFB			7.00 (080619)	17.40 (081900)
Andersen NASA	7.67 (080600)	13.69 (080600)	14.60 (080600)	20.68 (081400)
Sinajana				18.48
Mangilao	6.58 (080600)	15.39 (080700)	22.48 (080900)	25.61 (090200)
Windward Hills 1	6.18 (080600)	15.09 (080800)	18.55 (080900)	20.11 (~9-hr)
Inarajan DanDan				~11 (090152)
Merizo				3.73 (090152)
USGS (Prelim)				
Dededo	2.88	6.00	7.44	12.84
Umatac	1.32	2.88	4.20	6.00
Mt. Jumalong	2.40	5.76	7.80	10.44
Alamagosa	2.76	5.88	7.80	10.80
Mt. Chachao	4.92	11.22	13.63	15.84
Fena Reservoir	4.20	9.48	13.20	16.08
Windward Hills 2	4.08	9.84	12.60	15.48
Mt. Chachao	4.92	11.22	13.63	15.84

f. Storm Surge: The maximum storm surge and inundation (height of run-up) appears to be about 18 feet at coastal areas on eastern Guam, mostly from the swells generated by the approaching storm. Waves were likely 25-30 feet on the 50 to 600-foot cliffs of northeast Guam. On western shores, while the waves were not as high, due to the lower near shore elevations, the inundation and impact to the island was greater. Over all, the height of the storm surge on western windward coastlines ranged from 8 to 13 feet. These heights are consistent with a Category 4 typhoon on Guam. Many businesses in Hagatña had standing water as high as 3-4 feet. The War in the Pacific National Park in Asan had standing water in the Garage The wave action heavily damaged several sea walls and a few stretches of coastal roadways. In addition, there was a lot of deep coastal erosion on the west side of the island. The storm surge observed at selected locations on Guam is shown in Figure 9.

g. Satellite data: Figure 10 shows Dvorak satellite intensity analyses from two different objective techniques, one by the Zehr technique and one by the Velden-Olander technique. In practice, the Zehr technique gives values about 0.5 T-number too high, but the trends are good. Thus, in the figure, 0.5 T-number has been subtracted from each of the Zehr values. Two important pieces of information can be derived from the analyses, the absolute value of the T-number and the trend of the T-number. In the case of Pongsona, the T-number represents the current intensity, which can be given a discrete wind value. In the Dvorak technique, a T-number of 6.0 is equivalent to 115 knots (132

mph), a T-number of 6.5 is equivalent to 127 knots (146 mph), and a T-number of 7.0 is equivalent to 140 knots (161 mph). Figure 11 is a visual image of Typhoon Pongsona as it was approaching Guam about 75 n mi (86 mi) to the southeast. Figure 12 is a visible meteorological satellite image that shows Pongsona as it was traversing Guam at 0631 UTC. Figure 13a and 13b are microwave images of Pongsona nearly over Guam at 0422 UTC, and at its maximum intensity at 1235 UTC, respectively. These images illustrate the deep structure of the eye wall cloud, especially on the west side, which was likely the most intense part of the typhoon. This part of the typhoon passed over Guam. The objective Dvorak analyses indicate that Pongsona's peak intensity of 130 knots (150 mph) occurred at 1300 to 1400 UTC, after the eye wall cloud had moved northwest of the island (Figure 10). Based on the satellite analyses, the maximum intensity of the storm while it was over Guam was likely 120-125 knots (138-144 mph).

h. Radar data: The radar analysis was accomplished in much the manner of Stewart and Lyons (1996). Figure 14a is the reflectivity from the Andersen Air Force Base WSR88-D just before the radar lost power as the eye entered the island. Note that the western side of the eye wall cloud was already over Guam, but that the north side was not yet over Rota. The data also show that the eye wall cloud is much thinner on the northeast and southeast quadrants. Some of this is likely the result of attenuation from the heavy rain between the radar and the eastern side of the eye wall cloud. In fact, the satellite microwave data in Figure 13 confirms this. The animated radar data indicated that the eye was getting smaller as it approached Guam. While some of the reduction may have been actual shrinking of the eye, suggesting some intensification, a portion of the reduction was due to the radar looking at lower portions of the typhoon as it moved closer to the radar. Figure 14b is the velocity data at the same time. These data indicate that there were both inbound and outbound winds aloft that exceeded 128 knots (147 mph). While the actual value of winds above 128 knots (147 mph) could not be identified, the maximum wind could be estimated by applying a wind profile to the NEXRAD-observed wind speed thresholds. Wind profiles applied to the NEXRAD wind distribution yielded maximum winds of approximately 145-150 knots (167-173 mph) using the steepest plausible wind profile (Holland 1980) (i.e., $V R^{0.6}$ = constant, outside the radius of maximum wind; where V is wind speed and R is the radial distance from the center of the eye). The peak NEXRAD winds were located at an altitude of about 1000 ft (300 m). Experience has shown that the NEXRAD peak wind measurements tend to be representative of the gusts experienced at ground observing stations. The peak 1-minute sustained over-water wind associated with gusts of 145-150 knots is approximately 120-125 knots (138-144 mph).

i. Damage Assessment: A damage assessment of structures, infrastructure, and vegetation was conducted over most areas of the island. Several observations stand out. Neither on-site damage assessment nor inspection of aerial photographs taken by FEMA revealed any tornado activity.

1). Damage to structures: No Category 5-level damage was observed on the island. However, damage at the Guam Memorial Hospital and Perezville on Oka Point as well as at Two Lover's Point were mid Category 4-level, and the Lower and Upper Tumon areas

of Tumon Bay exhibited damage of low Category 4-level. Although there were no structural failures, several hotels lost glass windows and sliding doors. Some 44% of the island's 12,000 hotel rooms were rendered unusable following the typhoon, mostly from water damage.

Nevertheless, very widespread Category 4-level damage was observed over much of north central Guam, especially on the west side from Maite north to near Linguan Terrace in Dededo. Most of the damage was exacerbated by both the intensity and the duration of the winds. Several automobiles were violently flipped over, and several busses and other high profile vehicles were toppled by the wind (Figure 15a). A few tall baseball field light post were also toppled by strong winds; however, closer inspection showed the advanced stage of corrosion at the base of the metal light pole (Figure 15b). This type of corrosion was common to many posts supporting lights in parking lots and at outdoor sport facilities.

The most severe damage was to the older wooden structures weakened by wood rot or termite infestation, to concrete buildings with corrugated metal (tin) roofs, and to older or poorly constructed metal structures. Reinforced concrete frame buildings, reinforced concrete block walls, and well-designed and constructed metal structures were able to sustain the winds.

There was considerable glass breakage across the island, both in buildings and in automobiles. The window damage was widespread, primarily from the impact of flying debris and partly from the strong wind forces. Several windows covered with metal storm shutters imploded due to the high pressures caused by the wind gusts. Flying debris tore off some typhoon shutters. Not since Typhoon Pamela in 1976, has there been so much glass breakage. However, in the case of Pongsona, there were many more typhoon shutters in place and higher-wind load resistant glass had been installed in numerous structures.

a) Guam Memorial Hospital. The damage to the interior portions of the hospital (emergency room, pediatrics, and intensive care) was due to a sudden build-up of tremendous wind pressures, resulting from the loss of glass doors (Figure 16a) during the peak of the typhoon passage; this breakage permitted the intrusion of strong winds into the rooms. It is postulated that the glass doors were impacted by flying debris. Internal dry-wall partitions were damaged by the high wind pressures (Figure 16b). Not many glass windows were damaged, and there was no visible damage to the building's main structural system.

b) Hotel. Flying debris damaged the balcony railings to some parts of a high-rise building facing Tumon Bay, but the doors opening on to those balconies were visibly still intact (Figure 17a). The lightweight concrete covering panels were ripped off an exterior column and a portion of this building also lost several lightweight exterior wall panels. However, it was not possible to verify the type and condition of the connectors; the photograph (Figure 17b) shows some rusted attachment points. There was no visible damage to the building's main structural system.

c) Hotel. A major hotel at Tumon Bay sustained severe broken glass windows facing the bay. The breakage permitted the winds to breach the building envelope and the sudden build-up of internal pressures damaged some of the hallway dry-board walls (Figure 18a) and blew out some of the lightweight external wall material (Figure 18b). Several windows and sliding glass doors at the lobby level were broken. There was no damage to the building's main structural system.

d) Hotel. Another hotel, at the northerly-end of Tumon Bay, sustained heavy losses to its vertical rolling doors facing the bay (Figure 19a). The increased wind pressure caused damage to the mezzanine floor area and ceiling, but there was no damage to the building's main structural system. Overall, the glass windows and doors of the rooms of this hotel were able to resist the wind forces adequately. However, the air-conditioning system for this hotel collapsed during the storm. It was noted that many of the supporting members and parts for this air-conditioning system were badly corroded and therefore they were not able to withstand the impact of the high wind loads (Figure 19b). Proper preventive maintenance against corrosion might have mitigated this failure.

e) Monument. The monument at the Two-Lovers Point was toppled by the strong winds even though it was supported by guy cables and anchored by steel posts (Figure 20a).

f) Single-Family Residences. Many of the older, wooden-frame buildings with corrugated metal roofing were destroyed by the strong winds. (Typhoon Chata'an in July had already damaged much of this building stock.) Wood rot, termite infestation, corrosion of the nail connections and hurricane clips, together with the intensity and duration of the storm, all contributed to the demise of these older structures (Figure 20b).

The reinforced concrete frame or reinforced concrete masonry homes resisted the onslaught of the winds very well. Except for occasional visible damage to roof tiles, and damaged windows and doors, these structures showed no signs of distress (Figure 21a and Figure 21b).

g) New Industrial Building. An unfinished large industrial warehouse was destroyed by the strong winds. Excepting for a portion of a still-standing reinforced masonry end wall, the whole structural system was lying on its side, and an automobile was flipped upside down on the huge paved open parking lot (Figure 22a and Figure 22b). According to neighbors, the vertical rolling bay doors at the loading area had not yet been installed, allowing the wind to freely enter the building. Interestingly, a reinforced concrete residence, on an elevated area downwind from the direction of the strong winds, was not the least bit damaged.

h) Industrial Building in Maite. Another industrial building along the cliff line in Maite was in an utter collapse stage. Upon close inspection, it was noted that the main structural rigid-frame members, beams, purlins and column base anchors were in advanced stages of rust. Many of the webs were rusted through (Figure 23a and Figure 23b). Also, it was

surmised that the failure mechanism was most probably initiated by the impact from a container that had been slammed against the side of the building. Metal roofing sheets were found in the vicinity of a reinforced concrete apartment building adjacent to the damaged structure; these sheets had been torn off another building about 200 meters away and carried by wind action to this location.

i) Hardware Store in Maite. An adjacent smaller reinforced concrete masonry building, housing a hardware store, with wooden rafters and corrugated metal roofing was also damaged by wind effects; despite this, major parts of the rafter system and the metal roofing were still in place. It was noted that the glass louvers were all blown away which would then have permitted the wind to penetrate the building and cause high upward pressures on the roof system.

j) Church in Sinajana. A steel reinforced masonry church in Sinajana received catastrophic damage to its wood and corrugated metal roof, when improperly installed storm shutters were breached and the front doors blew in. The sudden build-up of internal pressures caused the roof to separate from its supporting beams (Figure 24). Recently installed, well-engineered "storm-proof" windows were unscathed by the debris and increased pressures. The roof proved to be the weakest part of the structure. Similar damage occurred to a church in Mangilao.

2). Damage to infrastructure:

a). Power system: While the infrastructure was heavily damaged by the typhoon, no Category 5-level damage was observed; most of the damage was to the transmission part of the system. Damages to power generation amounted to about $2 million. Numerous un-guyed or rotted wooden poles were either blown down or snapped off. Numerous un-guyed hollow-spun concrete poles were blown down, dragged down, or sheared at various levels. A few of these poles that were un-guyed and set in concrete broke at the base. Several of the hollow-spun concrete poles were poorly constructed, and the pre-stressing steel cables were not embedded in the concrete, but bunched together in the hollow core (Photos Figures 25a and 25b). The authors observed no fallen concrete poles that were guyed, nor any downed or damaged steel or solid concrete poles. Over 715 power poles and 800 transformers on Guam were damaged by this storm. Many secondary lines were downed, but many of these lines were dragged down as the poles fell. Some 43,000 households and businesses were affected. Damage to the power distribution network amounted to more than $52 million. Ninety-nine percent of the power was restored within 2 months (PDN 2003).

b). Telephone system: While most of Guam's telephone lines are underground, the telephone system suffered the most damage since Typhoon Pamela in 1976. The main switching centers received heavy water damage, destroying numerous computer circuit boards required for efficient switching of telephone calls and for carrying wide band communications. In addition, there was heavy damage to the surface-mounted pedestals, where individual user lines are spliced to the major cables. As a result, more than 12,000 customers were without telephone service.

c). Water and waste-water systems: During Typhoon Chata'an's passage in July, many rivers flooded to levels not seen by long-time residents before. These swollen rivers scoured gorges, dislodging many old trees, and causing heavy erosion and numerous landslides. The heavy runoff from Pongsona into the Fena Watershed again caused considerable erosion (Figure 26a) and severe silting in the Fena Reservoir, making lake waters unsuitable for drinking water production for several days (Figure 26b). Water and waste-water services were knocked out to most of the island, primarily due to the loss of power and the failure of emergency generators. An assessment by the US Army Corps of Engineers indicated that direct storm damage to both systems was minimal, but that most of the experienced failures were due to poor preventive maintenance.

d). Other infrastructure components: One of the greatest impacts of the typhoon was a fire at the fuel farm at the commercial port (Figure 27a). The fire burned for five days, preventing distribution of gasoline across the island (and across much of Micronesia). This caused a severe gas shortage, greatly hampering recovery and delaying the acquisition of data for this assessment. The cause of the fire is unknown, but may have been started by lightning. Eyewitnesses reported that Typhoon Pongsona contained an extraordinary amount of lightning during its movement over Guam.

Coastal erosion washed out a few stretches of road and blocked several stretches of road with rubble and sand. Downed trees and power poles blocked numerous roadways, although most had been cleared by the time the assessment team had arrived. High winds caused sever damage to many communications towers, including several at a communications station in Barrigada (Figure 27b).

3). Damage to vegetation: The separation between dominant first winds and the dominant second winds are easily determined from an assessment of tree damage and tree falls. The zone of demarcation between dominant first-winds and dominant second-winds is shown in Figure 28. From the analysis, it is evident that most of the damage was related to the second wind. The biggest difficulty in performing the analysis was differentiating some of the Typhoon Pongsona damage from some of the Typhoon Chata'an damage and tree falls.

Many palm trees weathered the winds surprisingly well. Some palms lost their crowns, but not as many as expected, considering the strength of the winds. Many palms were blown down, but primarily because the heavy rains softened the ground sufficiently. Otherwise, many of these fallen trees might have been de-crowned. In coastal areas, many palm trees fell due to undermining by ocean waters. Many palms had twisted crowns, but these were often near multi-story buildings or risen elevations, where the winds accelerated and formed strong eddies. However, a large stand of palms in a relatively open area near Ritidian Point (northwest corner of Guam) had extensive twisting of the crowns, reflecting rapid wind shifts during eye passage of an intense cyclone (Figure 29). Brittle trees, such as mango, African tulip, and shower trees lost many large branches, and many large trees with large profiles were uprooted. There were widespread areas where vegetation was badly scoured, and where smaller bushy trees and

shrubs were flattened to the surface. The most severe flattening of these trees and shrubs occurred in the Perezville area, on the west side of the island on top of the cliff line between the Guam Memorial Hospital and Ypao Beach. Some severe scouring also occurred in hilly/mountainous areas where funneling or up- and down-slope wind accelerations occurred. The island had a general brown appearance, but with large patches of green, especially in the south. Overall damage to vegetation was consistent with that of a Category 3 typhoon with smaller areas of a Category 4 typhoon.

i. Overall intensity assessment: Based on all of the available data, the over-water intensity of Pongsona as it passed across Guam was 125 knots (144 mph) with gusts of 150 knots (173 mph). Typhoon Pongsona also exposed the most populated and developed part of the island to the strongest winds, with winds over 100 knots (115 mph) lasting more than 6 hours in some west coast locations. Often during these wind assessments, one or more of the components of the analysis falls outside the expected range of values, clouding the picture and increasing the uncertainty. However, in the case of Pongsona, all of the components fit nicely in to a very narrow 12-knot (14-mph) window of maximum wind speed, with a sharp peak at 125 knots (144 mph). Figure 30 is the final intensity analysis for the maximum wind gusts over Guam. Actual sustained winds over Guam, except at the extreme western coastal areas, cannot be determined because of the varying terrain, building, and surface-roughness effects. This figure is fairly representative of the peak gust distribution across the island, since the potential peak gust is not so harshly affected by the varying terrain, building, and surface-roughness effects. Figure 31 is the wind intensity in terms of Saffir-Simpson Tropical Cyclone Scale typhoon damage Category, given in one-half Category increments.

4. Rota

a. Eye Passage: Based on extrapolation of the radar data, satellite data, and other data obtained from the island of Rota, including several interviews, no eye passage occurred there. The most intense part of the eye wall cloud likely did not reach Rota Island, but remained just offshore in the Rota Channel (see Figure 2).

b. Wind Measurements: The Rota Airport is located on the northeastern part of the island. It is manned by Supplemental Aviation Weather Reporting Station (SAWRS) observers. On 8 December, during Typhoon Pongsona, the observers did not man the station. The HANDAR, also located at the Airport, measured maximum sustained winds at 0846 UTC on 8 December from 090º at 73 knots (84 mph) with gusts to 74 knots (85 mph). Typhoon-force winds were also observed during the following hour from 105º at 70 knots (81 mph) with gusts to 72 knots (83 mph). Winds were significantly higher on the southwestern and southern coasts. Winds on Rota varied only from east-northeast to southeast. There was no differentiation of first and second wind.

c. Pressure: The minimum sea-level pressure recorded at Rota was 965.5 hPa at 080847 UTC by the HANDAR. The lowest pressure during the following hour was nearly the same at 965.8 hPa. These pressures are significantly higher than the 937.1 hPa pressure observed on northern Guam, and suggest that this location on Rota was well outside the

eye and likely at the outer edge or outside the eye wall cloud. Applying the same pressure gradient as was observed over Guam between a 965 hPa pressure and the center of the eye would place the radius of maximum winds just west of Rota. It would also support 105 knot (121 mph) 1-minute over-water-equivalent sustained winds over Songsong Village.

d. Rainfall: Rainfall at Rota was not particularly heavy in northern sections, with a maximum 1-hour value of only 0.91 inches ending at 080745 UTC and a 24-hour value of 5.57 inches ending at 090245 UTC. This also suggests that this Rota location was just outside the eye wall cloud. Unquestionably, significantly more rain fell on southwestern, southern, and southeastern exposures, and over the Sabana area, however, no rainfall measurements were available in these regions. The USGS rain gauge on the Sabana was destroyed during Typhoon Chata'an in July 2002.

e. Storm Surge: A significant storm surge occurred on the southwest coast at Songsong Village. The surge was measured at 22 feet above normal tide. The surge ripped out the fuel pier and the pipeline that connects the pier to the elevated fuel tanks, destroyed a few homes, and flooded many other homes. The inundation of seawater crossed nearly four-fifths of the three-fourth-mile-wide isthmus on which Songsong Village is located. Figure 32 shows the effects of the 22-foot storm surge at Songsong Village.

f. Damage Assessment: Chip Guard of the NWS and Arthur Chiu of the University of Hawaii at Manoa performed a wind and damage assessment for determination of the maximum winds and other meteorological effects. The northern part of the island fared well, with OWE sustained winds at the village of Sinopalo Village estimated at 70-80 knots (81-92 mph) based on the level of damage to structures and vegetation. Winds to the north of Sinapalo Village, the airport and golf resort areas, were somewhat less, but still of typhoon force. However, winds on the south and west parts of the island were significantly stronger. Two large, newly constructed buildings appeared to endure the winds very well—the new high school at Sinopalo and the new Rota campus of the College of the CNMI on the northwest part of the island, which appeared to lose only a few ceramic roofing tiles.

A 1,600-foot escarpment, the Sabana, lies to the south of the airport, golf resort, and Sinopalo Village region. OWE maximum winds west of the Sabana ranged from 85-95 knots (98-109 mph), while those south of the Sabana and over most of Songsong Village were likely as high as 105 knots (121 mph), 1-minute sustained. Sustained winds as high as 110 knots (127 mph) could have affected the extreme southwestern coastal part of the Wedding Cake peninsula, but the extreme southwestern part of the peninsula was not visited. Few wooden structures in Songsong Village survived the winds without severe damage or total destruction (Figure 33). Concrete structures with concrete roofs fared well, but a large number of the concrete structures with wood and tin roofs lost part or all of their roofs. The duration of the strong winds over southern Rota is not known, but the short duration of typhoon-force winds at the Rota Airport suggests that the duration, even over southern Rota, was significantly less than it was over Guam. There was no indication of tornado activity on the island.

g. Satellite data: Satellite data indicated that the eye passed about 20 n mi (23 miles) west of Rota at about 1000 UTC. The radius of maximum winds was likely just a few miles of the southwestern part of the island. However, the eye wall cloud passed over southern parts of Rota. The maximum intensity of the typhoon at this time was 125-130 knots (144-150 mph). Figures 12 and 13 illustrate Typhoon Pongsona near Rota at maximum intensity.

h. Radar data: The WSR-88D on Guam failed at 0526 UTC on 8 December, before the maximum winds reached Rota. Radar data suggested that the eye wall cloud to the north and northeast was somewhat thinner and less well-developed than that to the south and west. However, some of the difference was likely due to attenuation by the heavy rain. Extrapolation of the Doppler radar data at 0526 UTC (Figures 14a and 14b) also suggests that the maximum winds in the north part of the eye wall likely passed just west of Rota.

i. Overall wind assessment: Based on all available data, Rota likely experienced maximum 1-minute sustained winds of 110 knots (127 mph) with gusts to 135 knots (155 mph), or the winds of a mid Category 3 typhoon on the extreme west coastal part of the island. However, at the southeastern coast of Songsong Village, the maximum 1-minute sustained winds were 105 knots (121 mph) with gusts to 130 knots (150 mph). This wind speed also corresponds to a mid Category 3 typhoon. Figure 34 shows the analysis of the peak gust, the typhoon wind damage Categories, and the tree fall direction over Rota.

5. Tinian and Saipan

a. Track: Typhoon Pongsona passed west of Tinian and Saipan on 8 an 9 December. The typhoon center passed within 69 n mi (80 miles) of West Tinian Airport at about 1800 UTC on 8 December and within 79 n mi (90 miles) of Saipan International Airport at about 1300 UTC on 8 December. The radius of maximum wind extended about 25 n mi (29 miles) from the center at these times. At this time Typhoon Pongsona's intensity had peaked at 130 knots (150 mph) (see Figure 2).

b. Winds: The maximum sustained wind and peak gust observed at the Saipan International Airport were from 090º at 41 knots (47 mph) and 49 knots (56 mph), respectively, at 1129 UTC on 8 December. The maximum wind observed sustained wind at the West Tinian Airport HANDAR was from 103º at 35 knots (40 mph) at 1200 UTC on 8 December. The peak gust was from 112º at 35 knots (40 mph) at 1300 UTC and from 130º at 35 knots (40 mph) at 1500 UTC.

c. Pressures: The minimum observed sea level pressure at the Saipan International Airport was 995.7 hPa at 1129 UTC on 8 December. The minimum sea level pressure observed at the West Tinian Airport HANDAR was 992.7 hPa at 1200 and 1300 UTC on 8 December.

d. Rainfall: Rainfall at West Tinian Airport for 24 hours ending at 2100 UTC on 8 December was 2.54 inches. The rainfall at Saipan was not available.

e. Storm surge: Storm surge was not measured on Saipan or Tinian. However, based on lack of significant reports, the inundation height is thought to be 10 feet or less at coastal areas on the south and east coasts. These coasts are generally elevated cliff areas, well above the 10-foot level.

f. Flooding and mudslides: No flooding or mudslides were reported on Tinian or Saipan. However, based on historical data, it is possible that some flooding occurred on the west side of Saipan in low-lying areas.

g. Damages: According to preliminary Red Cross assessments, both Saipan and Tinian had 2 houses destroyed, 7 houses with major damage, and 8 houses with minor damage, each. Maximum winds on Tinian and Saipan were thought to be Tropical Storm Category B with winds, ranging from 44-63 knots (50-73 mph).

ACKNOWLEDGEMENTS

The members of the NOAA-NWS Meteorological Assessment Team would like to express their sincere appreciation to the many individuals and agencies that supported and provided input to this study. While it is impossible to name every person and agency, we would like to mention a few. Great appreciation goes to: the staffs of the Government of Guam and the Commonwealth of the Northern Mariana Islands (CNMI); the 36th Air Base Wing at Andersen Air Force Base and the Commander, Naval Forces Marianas; the Typhoon Pongsona FEMA Relief Team; and the staff of the Weather Service Forecast Office Guam. The team also wishes to extend its sincere thanks to Dr. Leroy Heitz, Mr. John Jocson and Ms. Theresa Hormillosa of the Water and Environmental Research Institute (WERI) at the University of Guam, and Ms. Maria Kottermair and Mr. Ernie Jillson for their invaluable assistance in producing some of the graphics for the study. Finally, the team would like to acknowledge the private sector businesses and the citizens of Guam and Rota for their cooperation and assistance in gathering invaluable and perishable information.

REFERENCES

Atkinson, G. D., and C. R. Holliday, 1977: Tropical cyclone minimum sea-level pressure and maximum sustained wind relationship for the western North Pacific. *Mon. Wea. Rev.*, **105**, 421-427.

Callaghan, J., and R. K. Smith, 1998: The relationship between maximum surface wind speeds and central pressure in tropical cyclones. *Australia Meteorological, Mag.,* **47**, 192-202.

Dickenson, M., and J. Molinari, 2002: Mixed Rossby-Gravity waves and Western Pacific tropical cyclogenesis. Part I: Synoptic Evolution, *J. Atmos. Sci*., **59**, 2183-2196.

Dvorak, V. F., 1975: Tropical cyclone intensity analysis and forecasting from satellite imagery. *Mon. Wea. Rev.*, **103**, 420-430.

Dvorak, V. F., 1984: Tropical cyclone intensity analysis using satellite data. NOAA Tech. Rep. NESDIS 11, 46 pp.

FEMA, (1993): Building Performance: Hurricane Iniki in Hawaii—Observations, Recommendations, and Technical Guidance. Federal Emergency Management Agency and Federal Insurance Administration, 100 pp.

Fujita, T. T., 1971: Proposed characterization of tornadoes and hurricanes by area and intensity. Satellite and Mesometeorology Research Project Research Paper 91, University of Chicago, 42 pp.

Fujita, T. T., 1992: The Fujita tornado scale, In "Mystery of Severe Storms", p. 31. Wind Research Laboratory Paper 239, Department of Geophysical Sciences, the University of Chicago, 298 pp.

Guard, C. P., M. P. Hamnett, C. J. Neumann, M. A. Lander, and H. G. Siegrist, Jr., 1999: Typhoon Vulnerability Study For Guam, *WERI Technical Report 85*, Water and Environmental Research Institute, University of Guam, Mangilao, Guam,156 pp.

Guard, C. P., and M. A. Lander, 1999: A Scale Relating Tropical Cyclone Wind Speed to Potential Damage for the Tropical Pacific Ocean Region: A User's Manual, *WERI Technical Report 86* (2nd edition), Water and Environmental Research Institute, University of Guam, Mangilao, Guam, 60 pp.

Holland, G. R., 1980: An analytical model of wind and pressure profiles in hurricanes. *Mon. Wea. Rev.*, **108**, 1212-1218.

Holton, J.R., 1992: The Planetary Bounday Layer. In, *An Introduction to Dynamic Meteorology*. Academic Press. New York, New York. pp 132.

Houston, S. H., G. S. Forbes, A.N.L. Chiu, 1999: The NOAA Super Typhoon Paka (1997) data acquisition team report, *Internal Report to the Working Group for Post-Storm Data Acquisition*, Office of the Federal Coordinator for Meteorological Services and Supporting Research, Silver Spring, MD, 1999.

Houston, S. H, G. S. Forbes, and A. N. L. Chiu, 2002: Impacts of Super Typhoon Paka's (1997) Winds on Guam: Meteorological and Engineering Perspectives," ASCE, *Natural Hazards Review*, **3**, pp 36-47.

JTWC, (editor F. Wells) 1991: Tropical Cyclones Affecting Guam (1671-1990). NOCC/JTWC Tech Note 91-2. US Naval Oceanography Command Center/Joint Typhoon Warning Center, Naval Oceanography Command Center, Stennis Space Center, MS. 45 pp.

Kraft, 1961: The hurricane's central pressure and highest wind. *Mariner's Weather Log*, **5**, 157.

Krayer, W. R., and R. D. Marshall, 1992: Gust factors applied to hurricane winds. *Bull. Amer. Meteor. Soc.*, **73**, 613-617.

Lander M. A., 1990: Evolution of the cloud pattern during the formation of tropical cyclone twins symmetrical with respect to the equator. *Mon. Wea. Rev.*, **118**, 1194-1202.

Lander, M. A., 1994: An exploration of the relationships between tropical storm formation in the western North Pacific and ENSO. *Mon. Wea. Rev.*, **122**, 636-651.

Lander, M. A., and C. P. Guard, 1997: High wave events: NAVSTA Family Housing Project. Prepared for Moffatt & Nichol Engineers, Long Beach, CA, 65 pp.

Marshall, T. P., 2002: Tornado damage survey at Moore, Oklahoma. *Wea. Forecasting*, **17**, 582-598.

PDN, 2003: *Pacific Daily News*, 4 Jan 2003, Gannett Publishing, pp. 1.

Powell, M. D., and S. H. Houston, 1996a: Hurricane Andrew's landfall in south Florida. Part I: Standardizing measurements for documentation of surface wind fields. *Wea. Forecasting,* **11,** 304-328.

Powell, M. D., and S. H. Houston, 1996b: Hurricane Andrew's landfall in south Florida. Part II:Surface wind fields and potential real-time applications. *Wea. Forecasting,* **11,** 329-349.

Saffir, H. S., (1972): Evaluation of structural damage caused by hurricanes. Phase 1, Final Report. National Science Foundation, Washington, D. C.

Simpson, R. H., 1974: The hurricane disaster potential scale. *Weatherwise*, **27**, 169-186.

Stewart, S. R., and S. W. Lyons, 1996: A WSR-88D radar view of Tropical Cyclone Ed. *Wea. Forecasting*, **11**, 115-135.

Velden, C. S., T. L. Olander, and R. M. Zehr, 1998: Development of an objective scheme to estimate tropical cyclone intensity from digital geostationary satellite infrared imagery. *Wea. Forecasting*, **13**, 172-186.

List of Figures

Figure 10. Intensity analysis of meteorological satellite imagery using Zehr's Digital Dvorak (DD) technique: maximum possible T number minus 0.5 T-number (triangles); and, the Velden-Olander Objective Dvorak Technique (ODT): 3-hour moving average (squares). The respective polynomial best-fit curves are also shown. Black oval indicates the intensity range with a peak near 123 knots (142 mph) as the eye of the typhoon exited the island.

Figure 11. . MODIS (moderate resolution imaging spectroradiometer) visual imagery 072222 UTC December 2002 of Typhoon Pongsona as it approaches Guam, with 115-knot (132-mph) sustained winds. The center of the eye is about 75 n mi (86 miles) southeast of Guam. (Courtesy of Chris Velden, Cooperative Institute for Meterological Satellite Studies, University of Wisconsin).

Figure 12. GMS-5 visual imagery at 080631 UTC December 2002 of Typhoon Pongsona as it passed across Guam, with 125-knot (144-mph) winds. The center of the eye is about 10 n mi (12 miles) east of northern Guam. (Courtesy of the Naval Research Laboratory, Monterey, CA).

Figure 13. TRMM horizontally polarized 85GHz imagery at (a) 080422 UTC December 2002, and (b) at 081235 UTC December 2002. The red area indicates the deep part of the eye wall cloud. The black within the red indicates cold-top temperatures colder than -94ºC. When over Guam (image (a)), the eye wall cloud contained frequent lightning. The 130-knot (150-mph) peak intensity of Typhoon Pongsona occurred close to the time of image (b).

Figure 14. Andersen Air Force Base WSR-88D at 080526 UTC December 2002 **(a)** reflectivity data and **(b)** velocity data of Typhoon Pongsona as it was just east of the island. For the reflectivity data, yellow indicates deep convection (heavy rains), primarily in the eye wall cloud, and red signifies the deepest convection (heaviest rains). For the velocity data, the inner green shade indicates inbound winds in excess of 128 knots, and the inner red indicates outbound winds in excess of 128 knots. The radar lost power just after these images were obtained.

Figure 15. (a) Toppled bus in Tamuning, Guam. **(b)** Toppled light pole at the Paseo baseball field in Hagatna, Guam. Note thinness of the rusted metal at the base.(NOAA Photos)

Figure 16. **(a)** Broken glass door at the Guam Memorial Hospital. **(b)** Dislodged internal wall in the pediatrics ward of the Guam Memorial Hospital. Assessment authors Chip Guard, Art Chiu, and Mark Lander appear from left to right.

Figure 17. (a) A major hotel in Lower Tumon. Note the in-tack doors leading to the balconies. **(b)** Missing lightweight exterior wall panels of a lower Tumon hotel, with very small rusted attachment points of connectors and the appearance of glue residue. (NOAA Photos)

Figure 18. (a) Blown in interior wall of a major Upper Tumon hotel. **(b)** Blown out exterior wall of a major Upper Tumon hotel. (NOAA Photos)

Figure 19. (a) Severely damaged typhoon doors of a major Upper Tumon hotel. **(b)** Severely rusted and corroded frame and connectors of one of the air conditioning units at a major Upper Tumon hotel. (NOAA Photos)

Figure 20. (a) Toppled statue at Two Lover's Point. Note failure of guy wires. **(b)** Severely damaged wood-rotted and termite-infested wooden house in Maite. (NOAA Photos)

Figure 21. (a) Concrete buildings held up well except for the loss of doors and windows. Wooden buildings sandwiched between concrete buildings did not fare so well. (NOAA Photo) **(b)** While storm shutters played a very important role in reducing water damage in buildings, they occasionally were victims of flying debris. (Photo by Carman Lujan)

Figure 22. (a) Nearly completed warehouse in Macheche, Dededo with reinforced concrete wall still standing. **(b)** Same building from another angle showing total destruction of the side walls and roof structure. (NOAA Photos)

Figure 23. (a) Industrial building near the cliff line at Maite. **(b)** Same building from another angle. Note overturned container that may have helped to destroy the building. (NOAA Photos)

Figure 24. (a) St. Judes Church in Sinajana, exterior view. **(b)** St. Judes Church, interior view.

Figure 25. (a) Damage to hollow-spun concrete power poles at Tanguissan Road. **(b)** Some hollow-spun concrete power poles were improperly constructed with the pre-stressing steel cables bundled down the hollow center instead of being imbedded in the concrete.

Figure 26. (a) Erosion and debris accumulation at a bridge, due to record rainfalls in central parts of Guam. (NOAA Photo) **(b)** Silt and debris in the Fena Reservoir on the US Naval Magazine following Typhoon Pongsona. (Official Navy Photos by JO1 Melody Kight Courtesy of COMNAVMAR)

Figure 27. (a) Fuel farm with burning tanks at the commercial port on Guam. Photo was taken 5 days after Ponsona's passage. (Official Navy Photos by JO1 Melody Kight Courtesy of COMNAVMAR) **(b)** High winds from Pongsona caused damage to several towers at a Communications facility in Barrigada (note the bent-over top of the tower located inside the black circle). (NOAA Photo)

Figure 28. Analysis of tree falls that occurred during Typhoon Pongsona. The green line separates areas where the "first wind" was dominant and areas where the "second wind" was dominant. Along the green line the two winds were equal in their dominance. Arrow size has no meaning.

Figure 29. (a) Splintered Australian pine trees at Ypao Beach, Lower Tumon, Guam near area of maximum wind. **(b)** Twisted crowns of coconut palms at Ritidian Point (NW Guam) indicating the rapid change in wind direction during eye passage. (NOAA Photos)

Figure 30. Analysis of peak gusts on Guam during the passage of Typhoon Pongsona on 8 December 2002. Winds are in miles per hour (MPH).

Figure 31. Pongsona peak wind distribution over Guam. Contours are in units of Saffir Simpson Tropical Cyclone Damage Scale (Guard and Lander 1999). Threshold gusts associated with each category are shown in the inset and in Appendix C.

Figure 32. (a) Near coastal effects of the 22-foot storm surge observed at Songsong Village, Rota. **(b)** Effects of the surge on the fuel-loading pipeline at Songsong, Rota. (NOAA Photos)

Figure 33. Destroyed wooden house and relatively unscathed reinforced concrete house in eastern Songsong Village, Rota, CNMI. (NOAA Photo)

Figure 34. Analysis of peak gusts (lower numbers), damage in terms of 0.5 Saffir-Simpson Tropical Cyclone Scale Category (upper numbers), and tree fall direction (blue arrows) for Rota, CNMI during the passage of Typhoon Pongsona on 8 December 2002.

Appendix A. Anemometer Information

Location	Instrument	Anemometer Type	Elevation	Averaging Period	Exposure	Peak Sustain (dir/kt/time UTC on 8 Dec)	Peak Gust (dir/kt/time UTC on 8 Dec)
Andersen AFB	AN/FMQ-13	Hot wire	10-meter tower	2-minute	open runway	030/41/0155	040/69/0227
Guam IAP	ASOS	3-cup	10-meter tower	2-minute	open runway	360/75/0501	350/102/0508
Guam IAP	F420	3-cup	6-meter tower	2-minute	open runway	270/92/0826	/100 pegged
Apra Harbor Tide Gauge	R. M. Young	Propeller	10-meter tower	2-minute	coastal; good	359/78/0700	354/101/0800
Cabras Island	HANDAR/F425A	3-prong ul-sonic	6-meter tower	2-minute	coastal; good	mis/42/0251	036/64/0051
Mangilao	HANDAR/F425A	3-prong ul-sonic	6-meter tower	2-minute	inland; fair	mis/75/0451	071/56/0251
Inarajan	HANDAR/F425A	3-prong ul-sonic	10-meter tower	2-minute	inland; good	mis/65/0351	213/81/0251
Merizo	HANDAR/F425A	3-prong ul-sonic	6-meter tower	2-minute	inland; poor	mis/44/0351	322/54/0251
Apra Harbor	Davis EasyMt	3-cup	10-meter roof	1-minute	inland; good	N/70/0530	N/110/0530
Sinajana	Davis EasyMt	3-cup	10-meter roof	1-minute	inland; fair	Not observed	NE/110/0550
Rota Airport	HANDAR/F425A	3-prong ul-sonic	10-meter tower	2-minute	open runway	090/68/0846	090/74/0846

Appendix B. Rain Gauge Information

Location	Owner	Rain Gauge Type	Elevation	Exposure	1-hr ending	3-hr ending	6-hr ending	12-hr ending	24-hr ending
Andersen AFB	USAF	12” manual	1-meter	open runway				7.00 080619	17.40 082354
Andersen AFB	NASA/U. Guam	7 dual recording 8” (14 total)	1-meter	inland; good	7.67 (80600)	13.69 (080600)	14.60 (080600)	19.60 (081200)	20.68 (081400)
Guam IAP	NWS	ASOS 8” recording	5-meter tower	open runway	miss	miss	miss	miss	miss
Guam IAP	NWS	8” manual	1-meter surface	inland; good			8.38	12.69	19.67 082354
Cabras Island	HANDAR NWS	8” recording	5-meter tower	coastal; good					miss
Mangilao	HANDAR NWS	8” recording	5-meter tower	inland; fair					9.61
Inarajan	HANDAR NWS	8” recording	1-meter surface	inland; good					~12.5 090152
Merizo	HANDAR NWS	8” recording	1-meter surface	inland; poor					3.73 090152
Agat Fire	NWS Coop	8” manual	1-meter surface	inland; fair					miss
Dededo	NWS Coop	8” manual	1-meter surface	inland; fair					miss
Mangilao Ag	NWS Coop	8” manual	1-meter surface	inland; fair					19.87 090000
Inarajan Ag	NWS Coop	8” manual	1-meter surface	inland; poor					miss
Yigo Animal	NWS Coop	8” manual	1-meter surface	inland; fair					miss
Sinajana	NWS spotter	8” manual	1-meter surface	inland; fair					18.48
Alamagosa	USGS preliminary	8” recording	3-meter	inland; good	2.76	5.88	7.80		10.80
Fena	USGS preliminary	8” recording	3-meter	inland; good	4.20	9.48	13.20		16.08
Mt Chachao	USGS preliminary	8” recording	3-meter	inland; good	4.92	11.22	13.63		15.84
Mt Jumalong	USGS preliminary	8” recording	3-meter	inland; good	2.40	5.76	7.80		10.44
Dededo	USGS preliminary	8” recording	3-meter	inland; good	2.88	6.00	744		12.84
Windward Hls	USGS preliminary	8” recording	3-meter	inland; good	4.08	9.84	12.60		15.48
Umatac	USGS preliminary	8” recording	3-meter	inland; good	1.32	2.88	4.20		6.00
Mangilao	U. Guam/NASA	8” recording	1-meter surface	inland; good	6.58 080600	15.39 080700	22.48 080900	24.79 (081200)	25.61 090200
Mangilao	U. Guam	4” manual	1.5-meter surface	inland; good	miss	miss	miss	miss	miss
Rota Airport	HANDAR NWS	8” recording	10-meter tower	open runway	0.91		3.98	4.81	5.57

Appendix C. Typhoon wind damage Categories in 0.5 divisions based on the Saffir-Simpson Tropical Cyclone Scale (Guard and Lander 1999).

Category	Threshold 1-min knots	Threshold gust knots	Threshold 1-min mph	Threshold gust mph
1.0	64	78	74	90
1.5	74	90	85	104
2.0	83	101	96	117
2.5	90	109	104	126
3.0	96	117	111	135
3.5	105	128	121	148
4.0	114	139	132	160
4.5	125	152	144	175
5.0	136	166	157	192

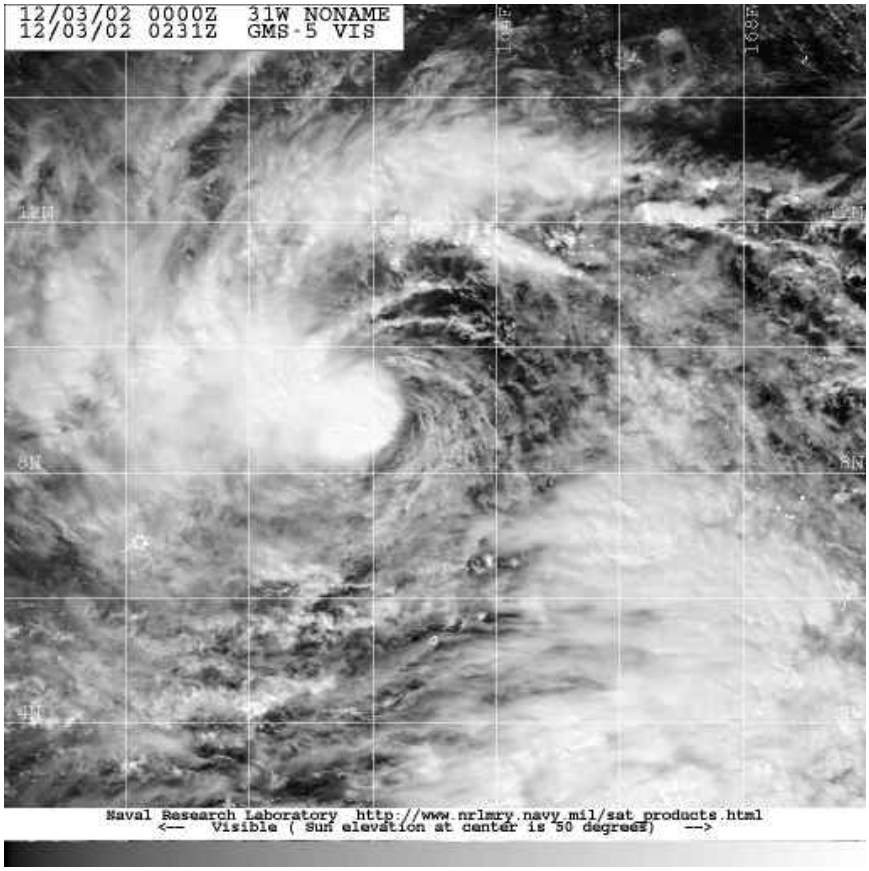

Figure 1. GMS-5 visual image at 030231 UTC December 2002of Tropical Storm Pongsona located about 260 nmi (300 miles) northeast of Pohnpei. The intensity is 35-40 knots (39-44 mph). (Courtesy Naval Research Laboratory, Monterey, CA)

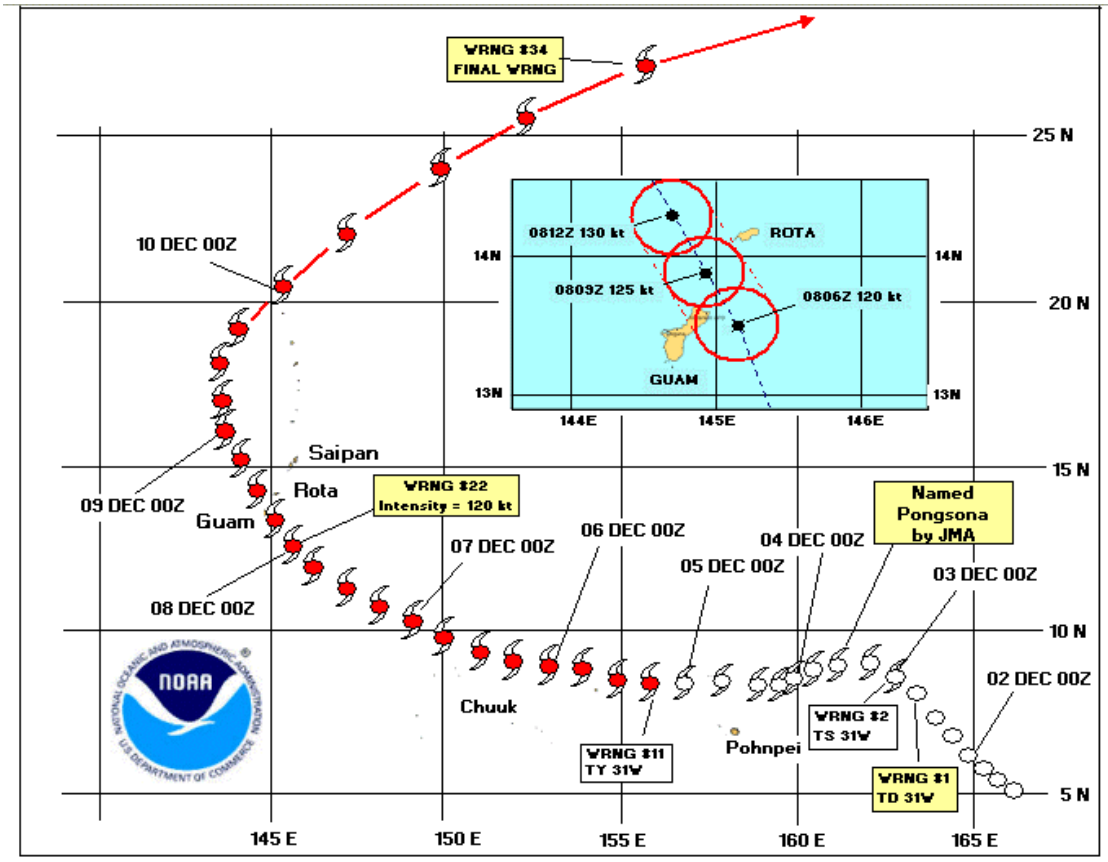

Figure 2. Best track of Typhoon Pongsona as it passed through Micronesia. Inset shows the 8 Dec 0600 UTC, 0900 UTC, and 1200 UTC positions as the eye passed over Guam and between Guam and Rota. Open circles indicate tropical depression intensity, open storm symbols indicate tropical storm intensity, and red storm symbols indicate typhoon intensity. The red circles in the inset indicate the extent of the eye.

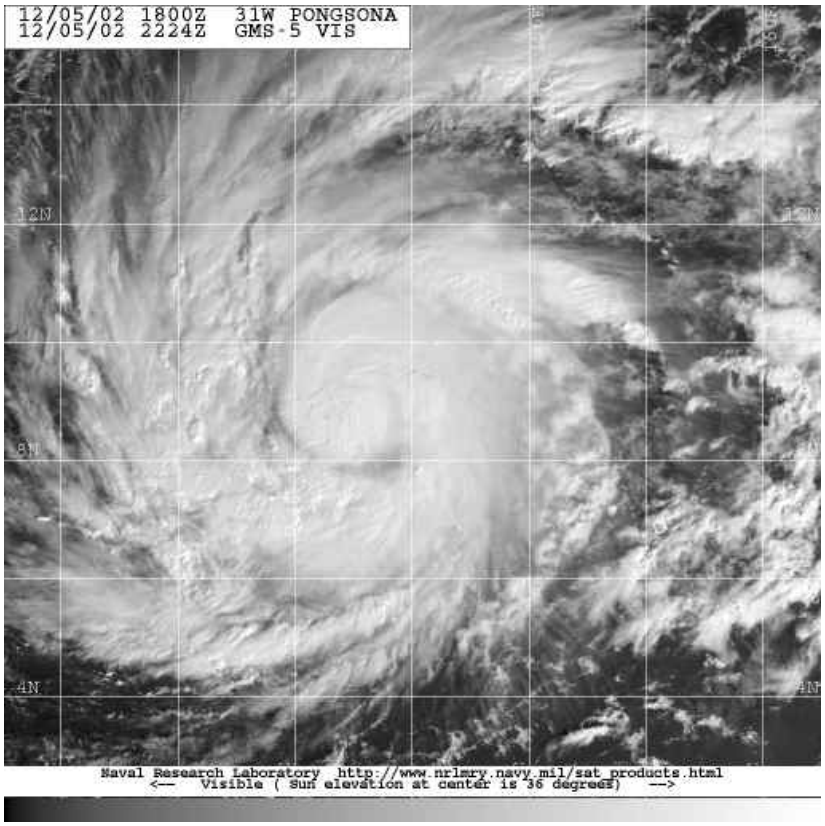

Figure 3. GMS-5 visual imagery 052224 UTC December 2002 of Typhoon Pongsona approximately 120 nmi (138 miles) north-east of Weno Island, Chuuk, with 70-75 knot (81-86 mph) winds. (Courtesy of the Naval Research Laboratory, Monterey, CA)

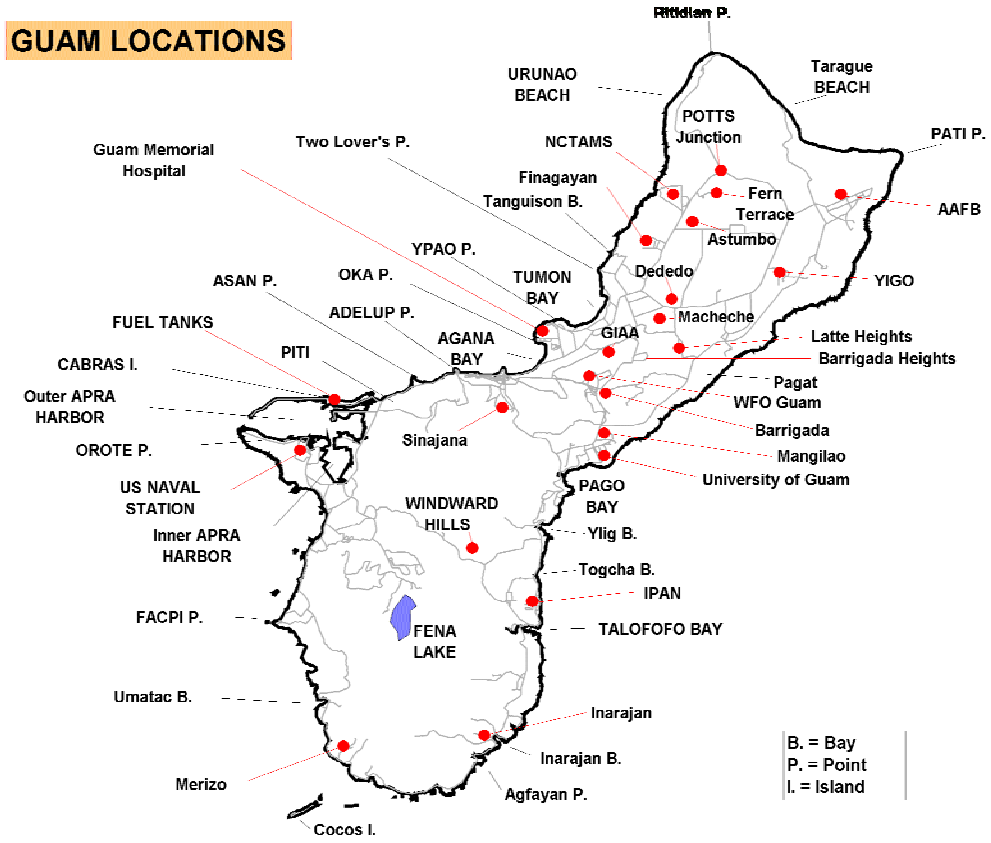

Figure 4. Map of Guam showing most of the locations discussed in the wind and damage analyses. (Map and GIS database courtesy WERI, University of Guam)

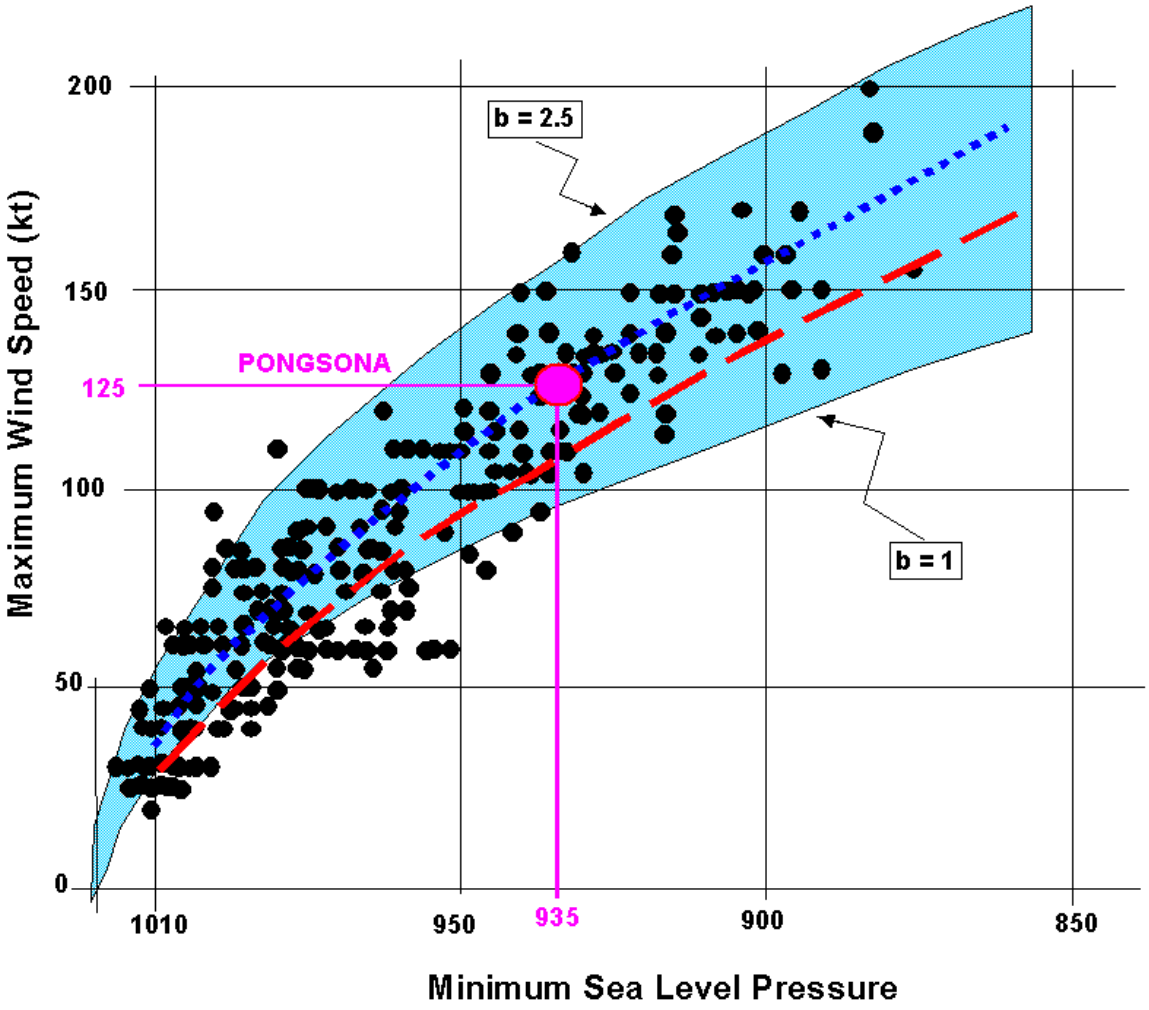

Figure 5. Relationship between maximum sustained wind and minimum sea-level pressure, where "b" values indicate theoretical limits of the relationship. Dots are actual aircraft reports for 1960's and 1970's prior to JTWC's use of the Atkinson-Holliday wind-pressure relationship (dashed line). Dotted line is the best-fit solution and is the relationship used for Typhoon Pongsona in this assessment. It is similar to the Kraft wind-pressure relationship used in the Atlantic.

(a) **(b)**

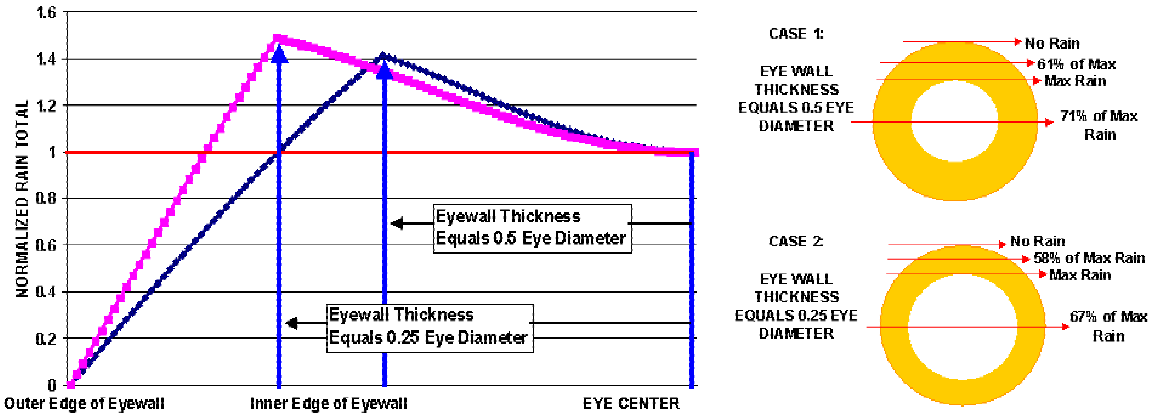

Figure 6. **(a)** Conceptual model of normalized rainfall distribution during eye passage of a typhoon, where the rainfall is related to eye wall cloud thickness and the eye diameter. **(b)** Schematic diagram shows rainfall expected as a function of path taken through eye wall. Case 1 illustrates a typhoon with a thick eye wall cloud and a small eye and Case 2 illustrates a typhoon with a thin eye wall cloud and a large eye.

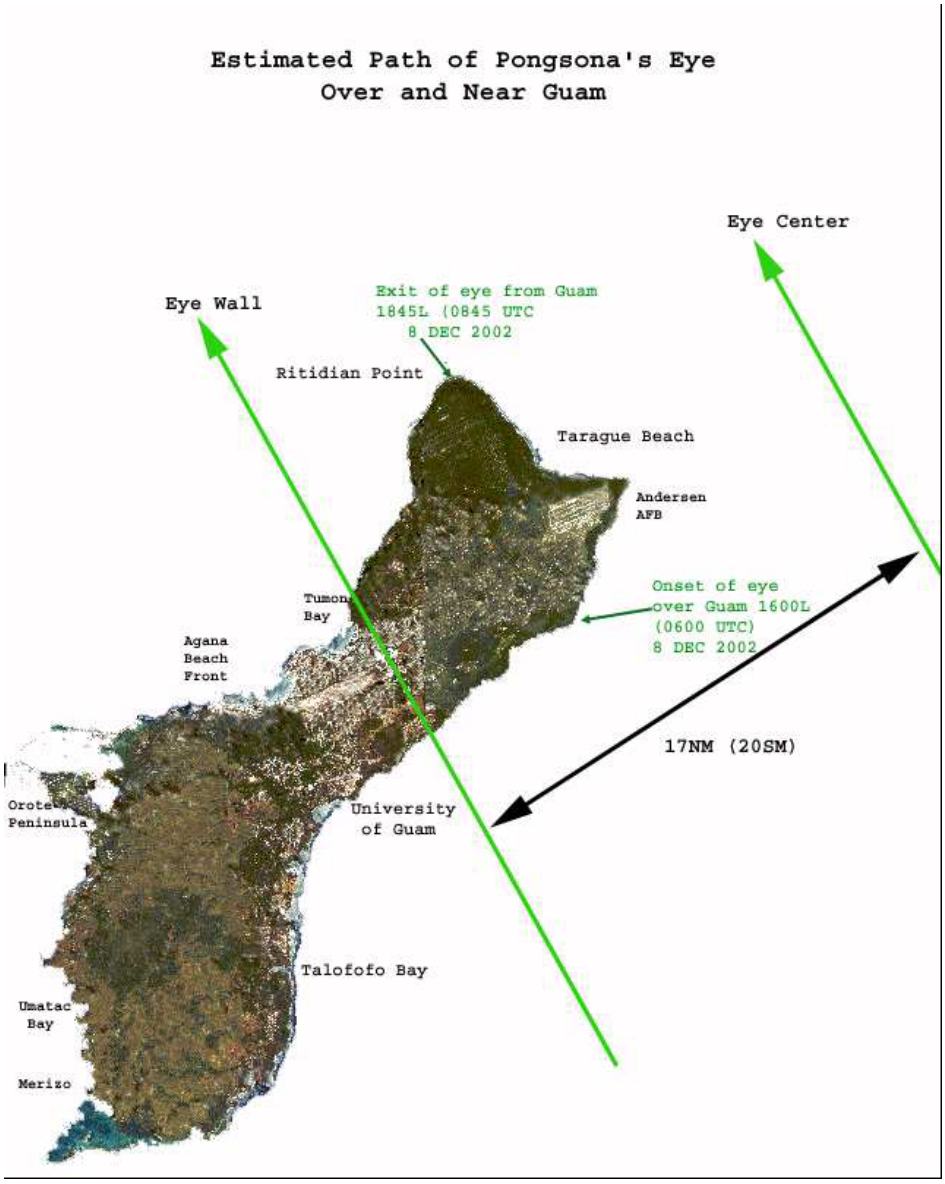

Figure 7. Track of Typhoon Pongsona's eye across Guam. The green line Labeled eye wall is the inner edge of the eye wall cloud.

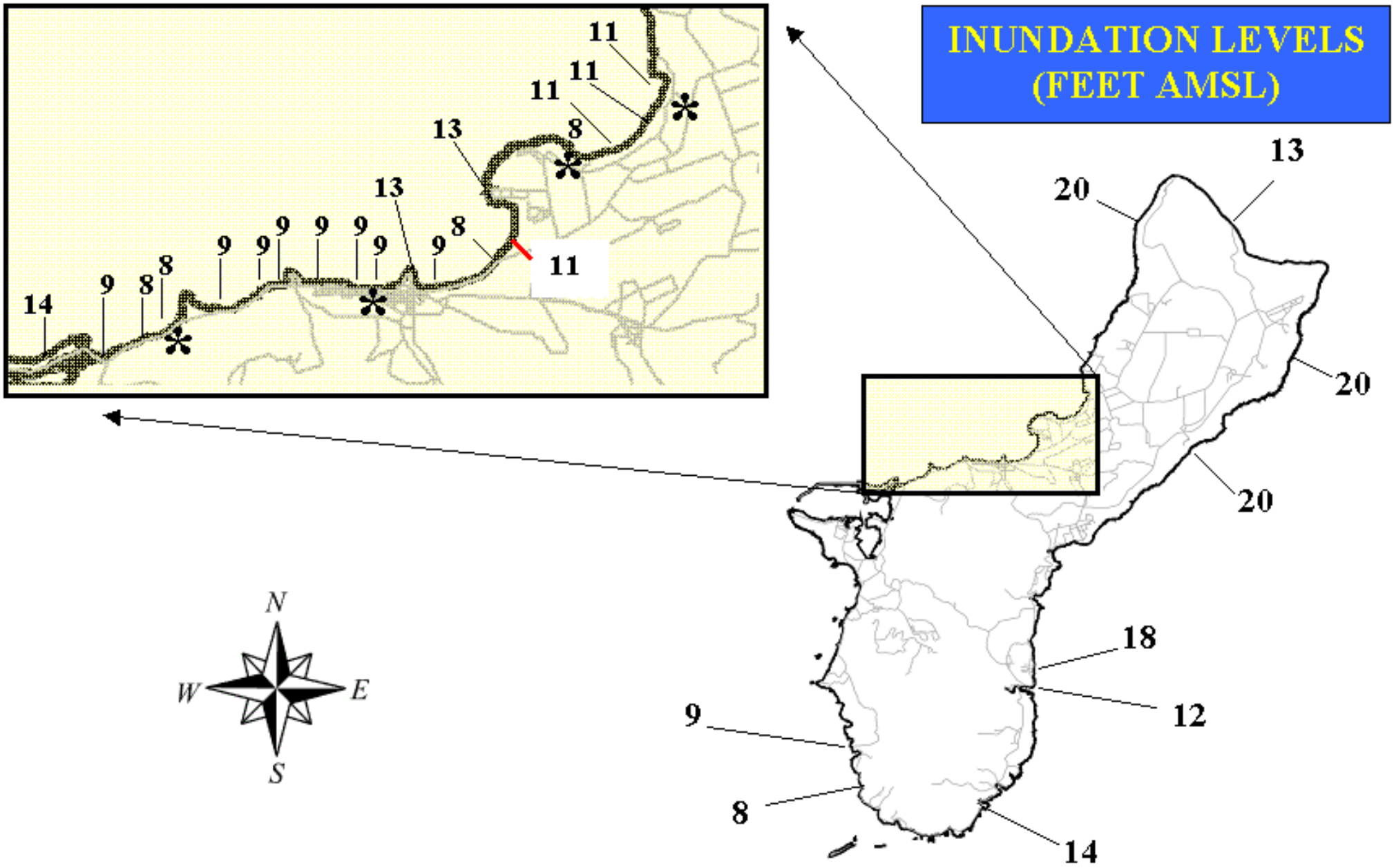

Figure 9. Heights (feet) of inundation of seawater above mean sea level (AMSL) at selected locations on Guam. Shaded area expands the area from the Commercial Port (extreme left) to Upper Tumon Bay (upper right). Asterisks (*) indicate measurements are from marks left by still water; otherwise, measurements are from debris edge of wave run-up.

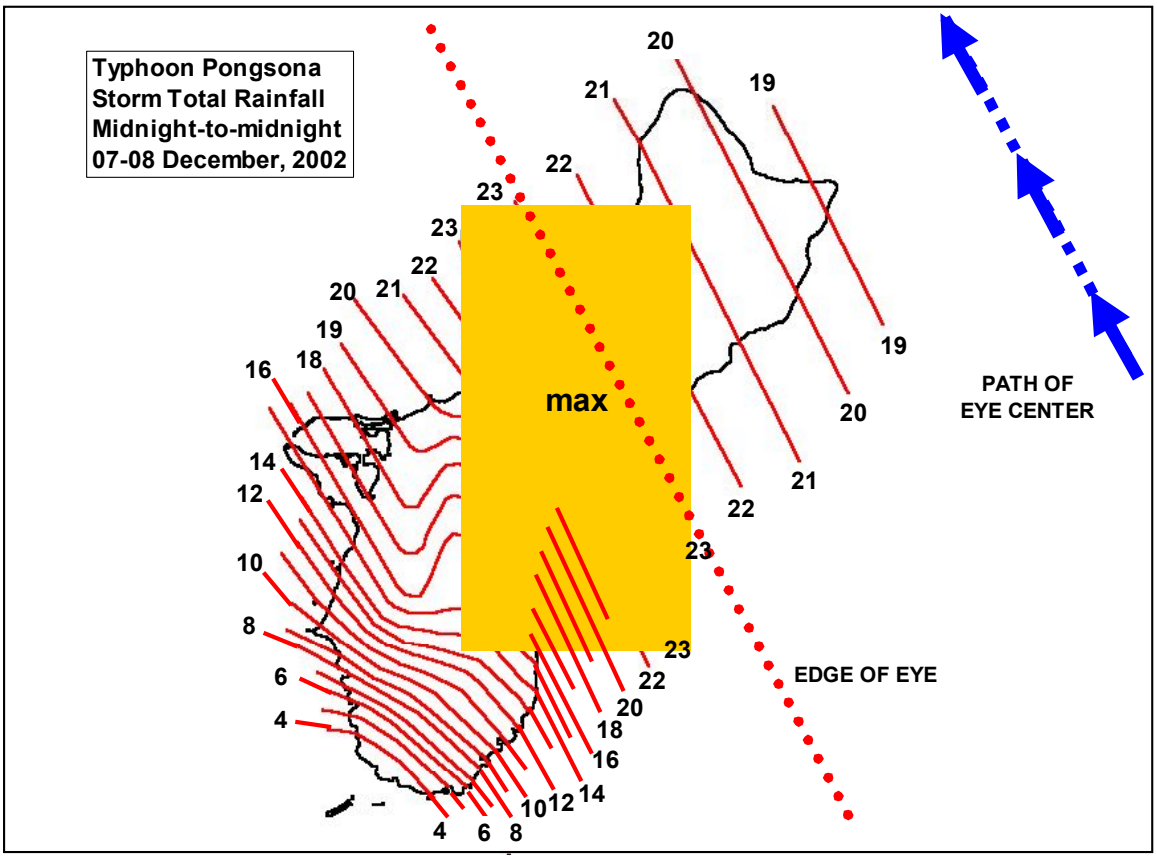

Figure 8. Analysis of 24-hour rainfall distribution in inches during the passage of Typhoon Pongsona over Guam.

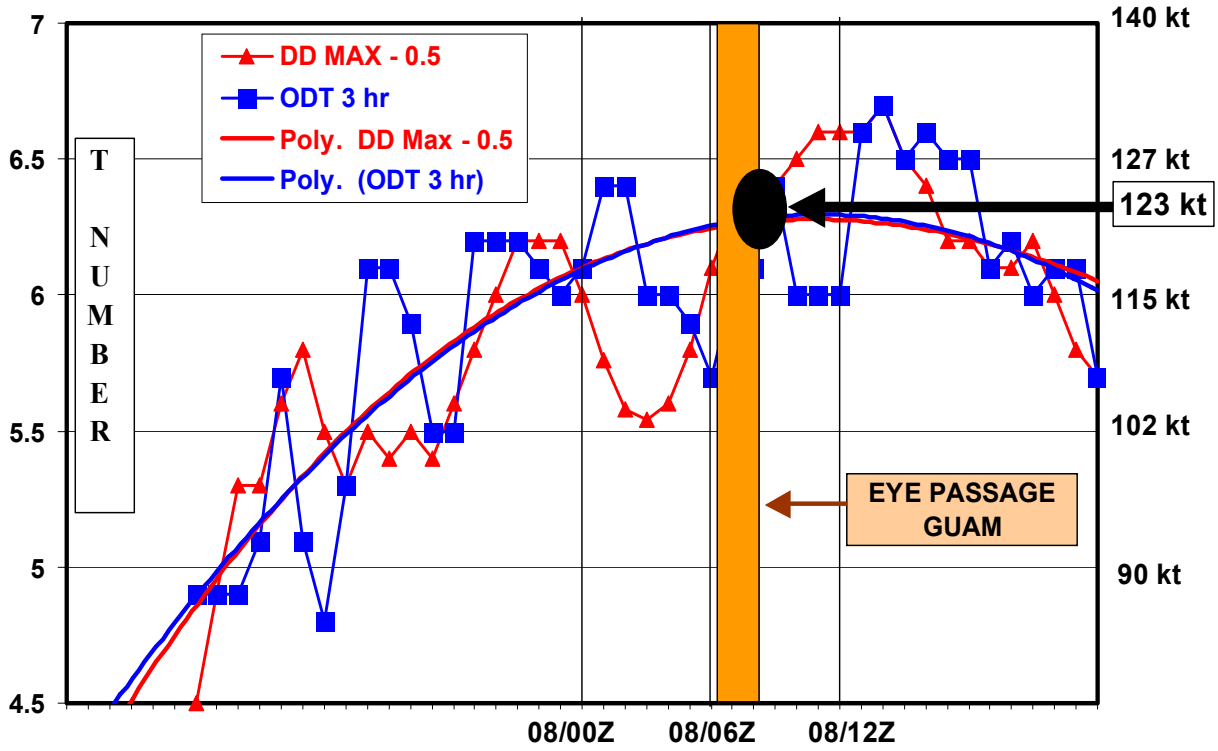

Figure 10. Intensity analysis of meteorological satellite imagery using Zehr's Digital Dvorak (DD) technique: maximum possible T number minus 0.5 T-number (triangles); and, the Velden-Olander Objective Dvorak Technique (ODT): 3-hour moving average (squares). The respective polynomial best-fit curves are also shown. Black oval indicates the intensity range with a peak near 123 knots (142 mph) as the eye of the typhoon exited the island.

Figure 11. MODIS (moderate resolution imaging spectroradiometer) visual imagery 072222 UTC December 2002 of Typhoon Pongsona as it approaches Guam, with 115-knot (132-mph) sustained winds. The center of the eye is about 75 n mi (86 miles) southeast of Guam. (Courtesy of Chris Velden, Cooperative Institute for Meterological Satellite Studies, University of Wisconsin).

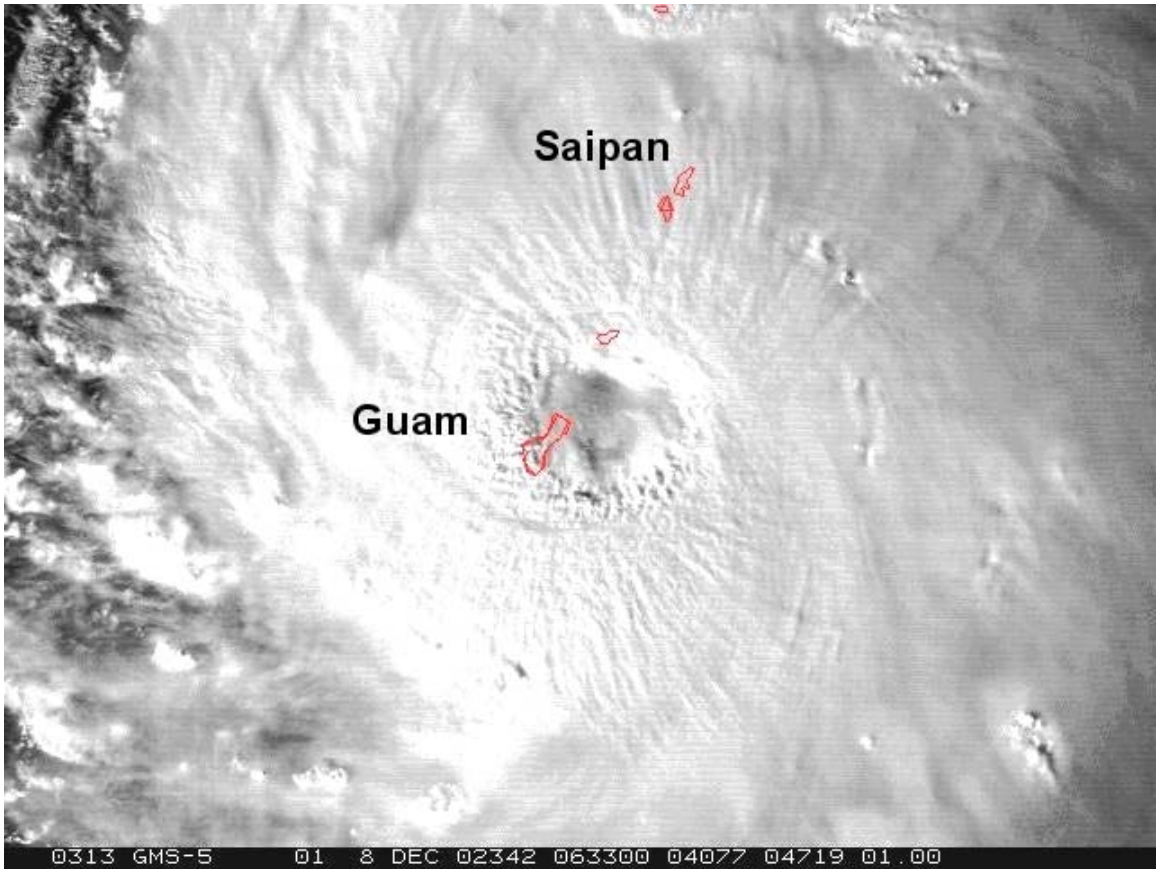

Figure 12. GMS-5 visual imagery at 080631 UTC December 2002 of Typhoon Pongsona as it passed across Guam, with 125-knot (144-mph) winds. The center of the eye is about 10 n mi (12 miles) east of northern Guam. (Courtesy of the Naval Research Laboratory, Monterey, CA)

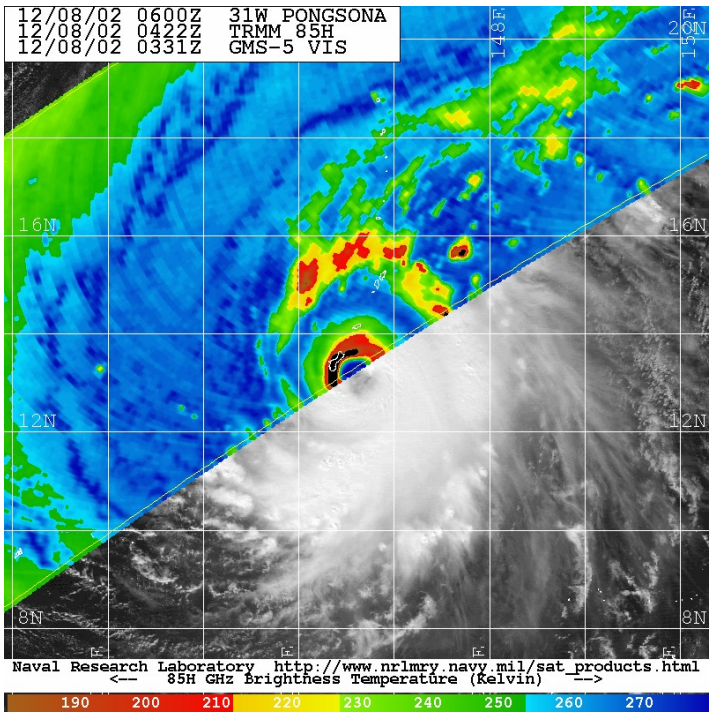

(a)

(b)

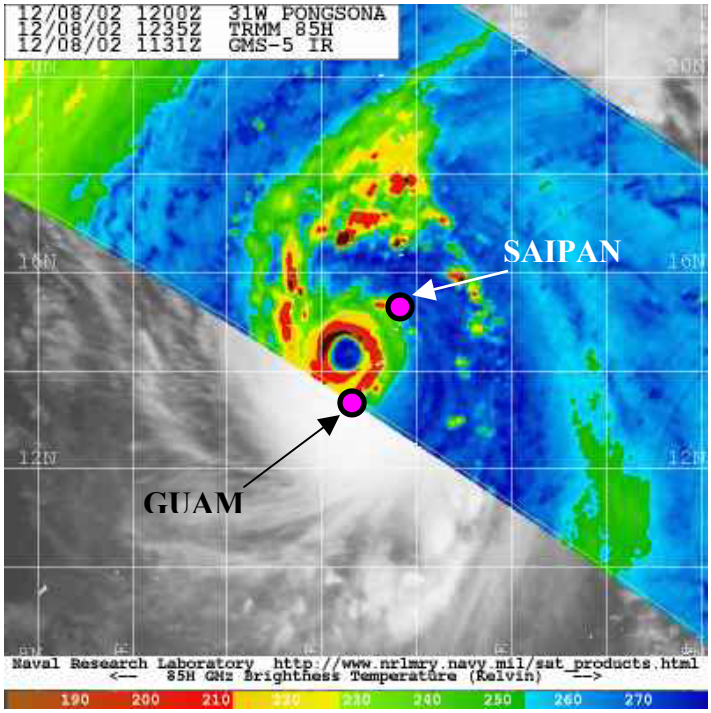

Figure 13. TRMM horizontally polarized 85GHz imagery at (a) 080422 UTC December 2002, and (b) at 081235 UTC December 2002. The red area indicates the deep part of the eye wall cloud. The black within the red indicates cold-top temperatures colder than -94ºC. When over Guam (image (a)), the eye wall cloud contained frequent lightning. The 130-knot (150-mph) peak intensity of Typhoon Pongsona occurred close to the time of image (b).

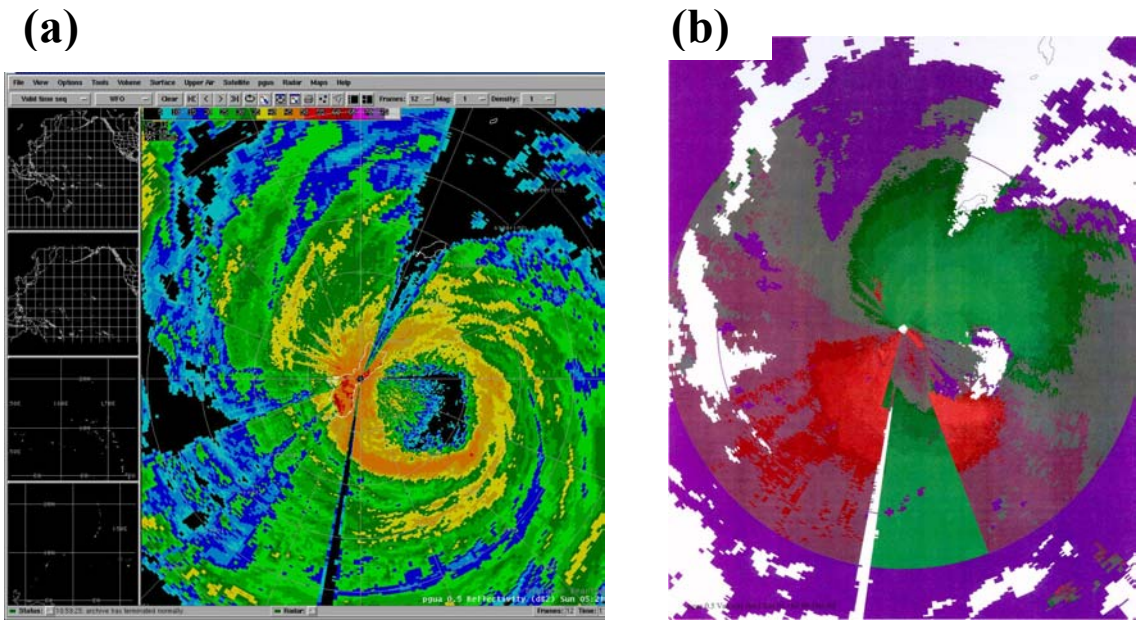

Figure 14. Andersen Air Force Base WSR-88D at 080526 UTC December 2002 reflectivity data (a) and velocity data (b) of Typhoon Pongsona as it was just east of the island. For the reflectivity data, yellow indicates deep convection (heavy rains), primarily in the eye wall cloud, and red signifies the deepest convection (heaviest rains). For the velocity data, the inner green shade indicates inbound winds in excess of 128 knots, and the inner red indicates outbound winds in excess of 128 knots. The radar lost power just after these images were obtained.

(a) **(b)**

Figure 15. **(a)** Toppled bus in Tamuning. **(b)** Toppled light pole at the Paseo baseball field. Note thinness of the rusted metal at the base.

(a) **(b)**

Figure 16. **(a)** Broken glass door at the Guam Memorial Hospital. **(b)** Dislodged internal wall in the pediatrics ward of the Guam Memorial Hospital. Assessment authors Chip Guard, Art Chiu, and Mark Lander appear from left to right.

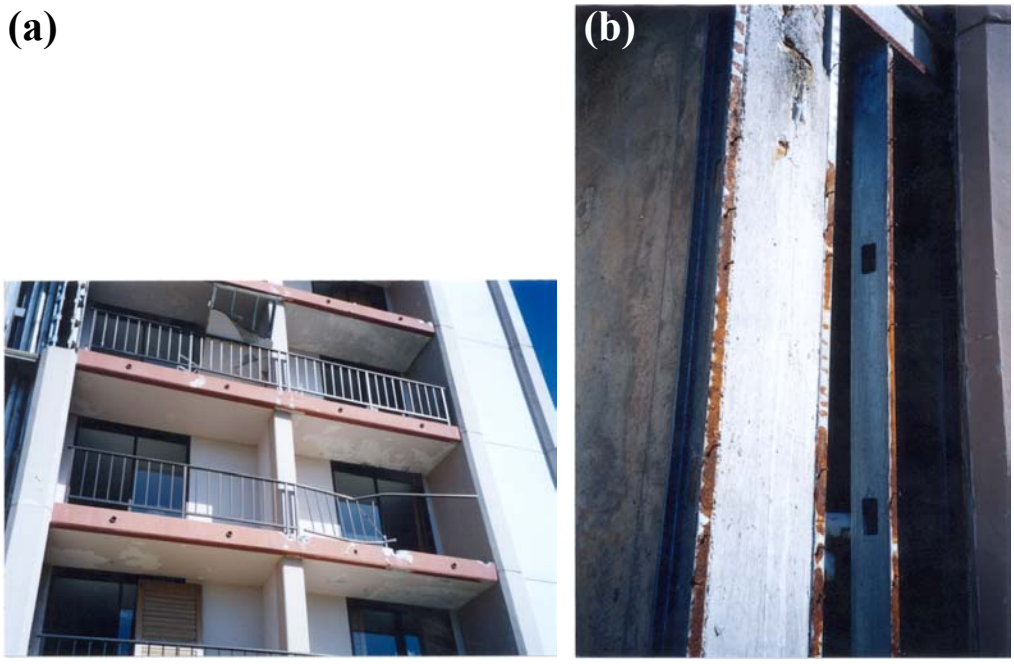

Figure 17. (a) A major hotel in Lower Tumon. Note the in-tack doors leading to the balconies. **(b)** Missing lightweight exterior wall panels of a lower Tumon hotel, with very small rusted attachment points of connectors and the appearance of glue residue. (NOAA Photos)**.**

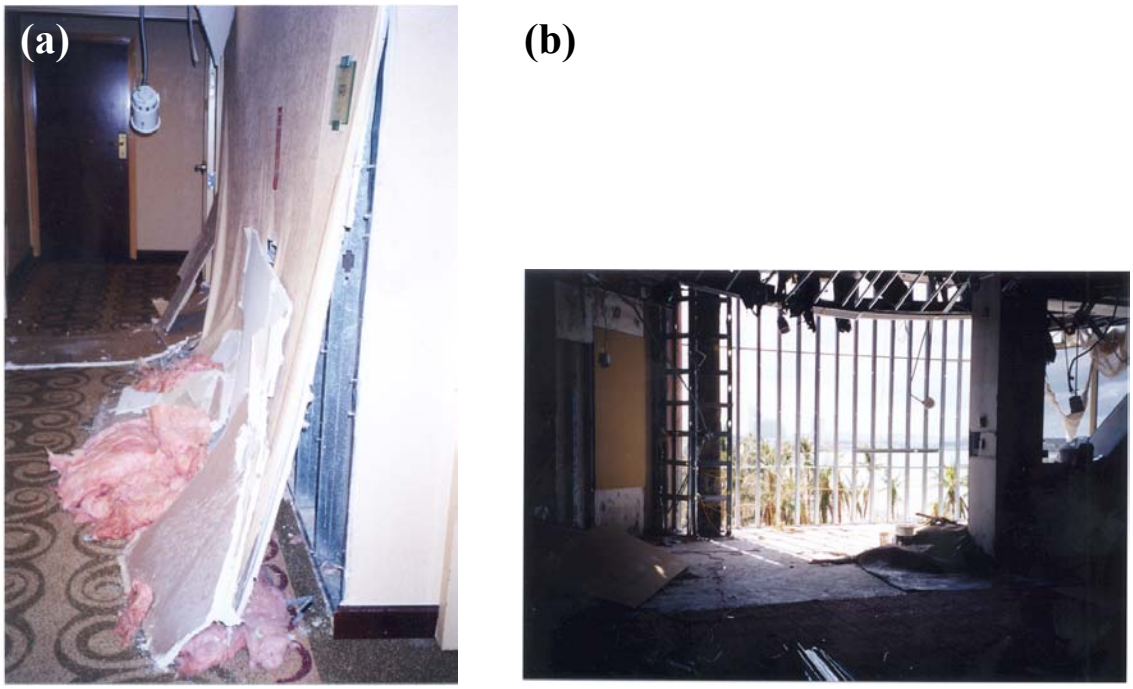

Figure 18. (a) Blown in interior wall of a major Upper Tumon hotel. **(b)** Blown out exterior wall of a major Upper Tumon hotel. (NOAA Photos)

(a) **(b)**

Figure 19. (a) Severely damaged typhoon doors of a major Upper Tumon hotel. **(b)** Severely rusted and corroded frame and connectors of one of the air conditioning units at a major Upper Tumon hotel.

(a) **(b)**

Figure 20. (a) Toppled statue at Two Lover's Point. Note failure of guy wires. **(b)** Severely damaged wood-rotted and termite-infested wooden house in Maite. (NOAA Photos)

(a) **(b)**

Figure 21. (a) Concrete buildings held up well except for the loss of doors and windows. Wooden buildings sandwiched between concrete buildings did not fare so well. (NOAA Photo) **(b)** While storm shutters played a very important role in reducing water damage in buildings, they occasionally were victims of flying debris. (Photo by Carman Lujan)

(a) **(b)**

Figure 22. (a) Nearly completed warehouse in Macheche, Dededo with reinforced concrete wall still standing. **(b)** Same building from another angle showing total destruction of the side walls and roof structure. (NOAA Photos)

(a) **(b)**

Figure 23. (a) Industrial building near the cliff line at Maite. **(b)** Same building from another angle. Note overturned container that may have helped to destroy the building. (NOAA Photos)

(a) **(b)**

Figure 24. (a) St. Judes Church in Sinajana exterior view. **(b)** St. Judes Church interior view. (NOAA Photos)

(a) **(b)**

Figure 25. **(a)** Damage to hollow-spun concrete power poles at Carnation Road in Latte Heights, Dededo. **(b)** Some hollow-spun concrete power poles were improperly constructed with the pre-stressing steel cables bundled down the hollow center instead of being imbedded in the concrete. (NOAA Photos)

Figure 26. (a) Erosion and debris accumulation at a bridge, due to record rainfalls in central parts of Guam. (NOAA Photo) **(b)** Silt and debris in the Fena Reservoir on the US Naval Magazine following Typhoon Pongsona. (Official Navy Photos by JO1 Melody Kight Courtesy of COMNAVMAR)

(a) **(b)**

Figure 27. (a) Fuel farm with burning tanks at the commercial port on Guam. Photo was taken 5 days after Ponsona's passage. (Official Navy Photos by JO1 Melody Kight Courtesy of COMNAVMAR) **(b)** High winds from Pongsona caused damage to several towers at a Communications facility in Barrigada (note the bent-over top of the tower located inside the black circle). (NOAA Photo)

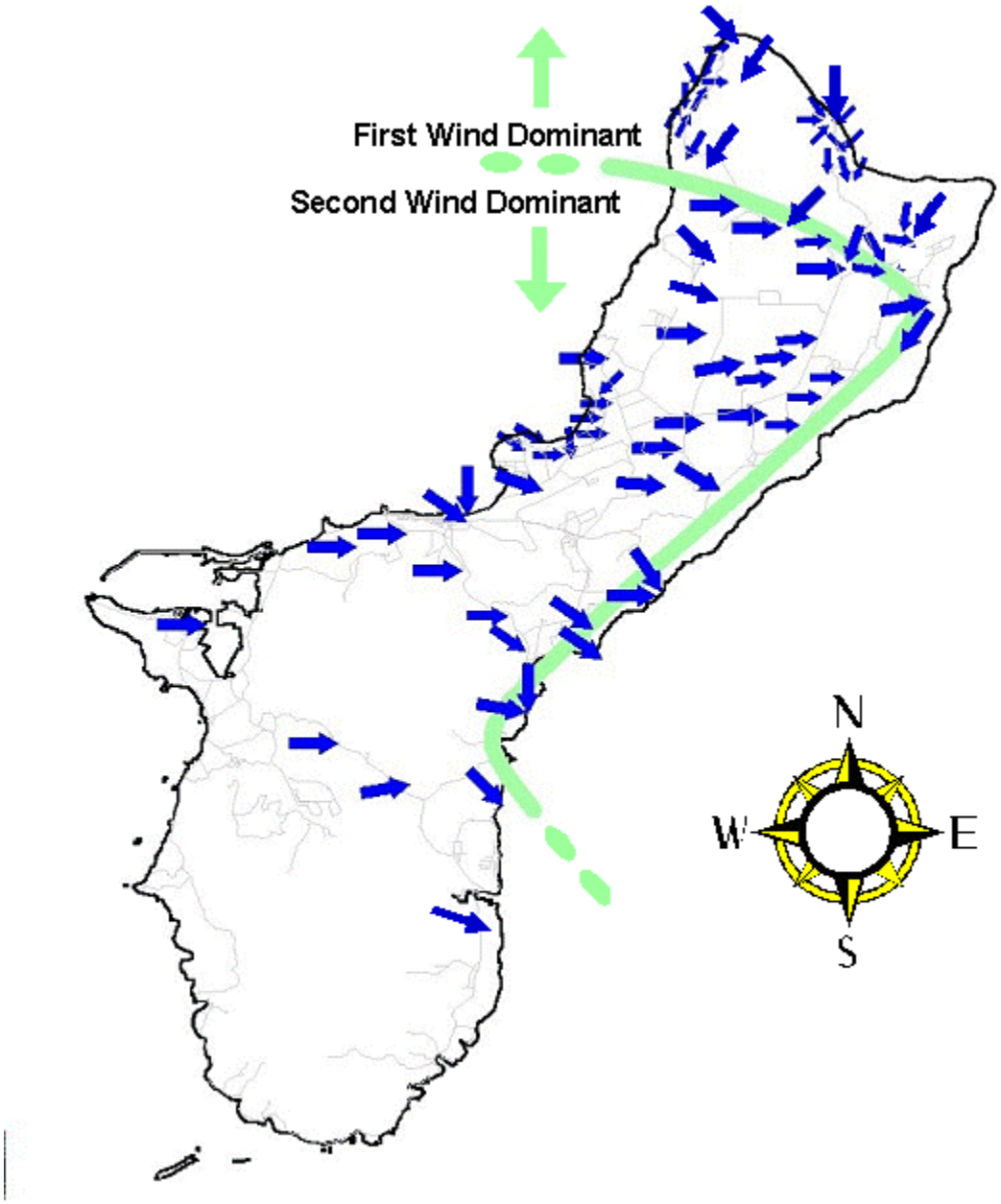

Figure 28. Analysis of tree falls that occurred during Typhoon Pongsona. The green line separates areas where the "first wind" was dominant and areas where the "second wind" was dominant. Along the green line the two winds were equal in their dominance. Arrow size has no meaning.

(a) **(b)**

Figure 29. **(a)** Splintered Australian pine trees at Ypao Beach, Lower Tumon, Guam near area of maximum wind. **(b)** Twisted crowns of coconut palms at Ritidian Point (NW Guam) indicating the rapid change in wind direction during eye passage. (NOAA Photos)

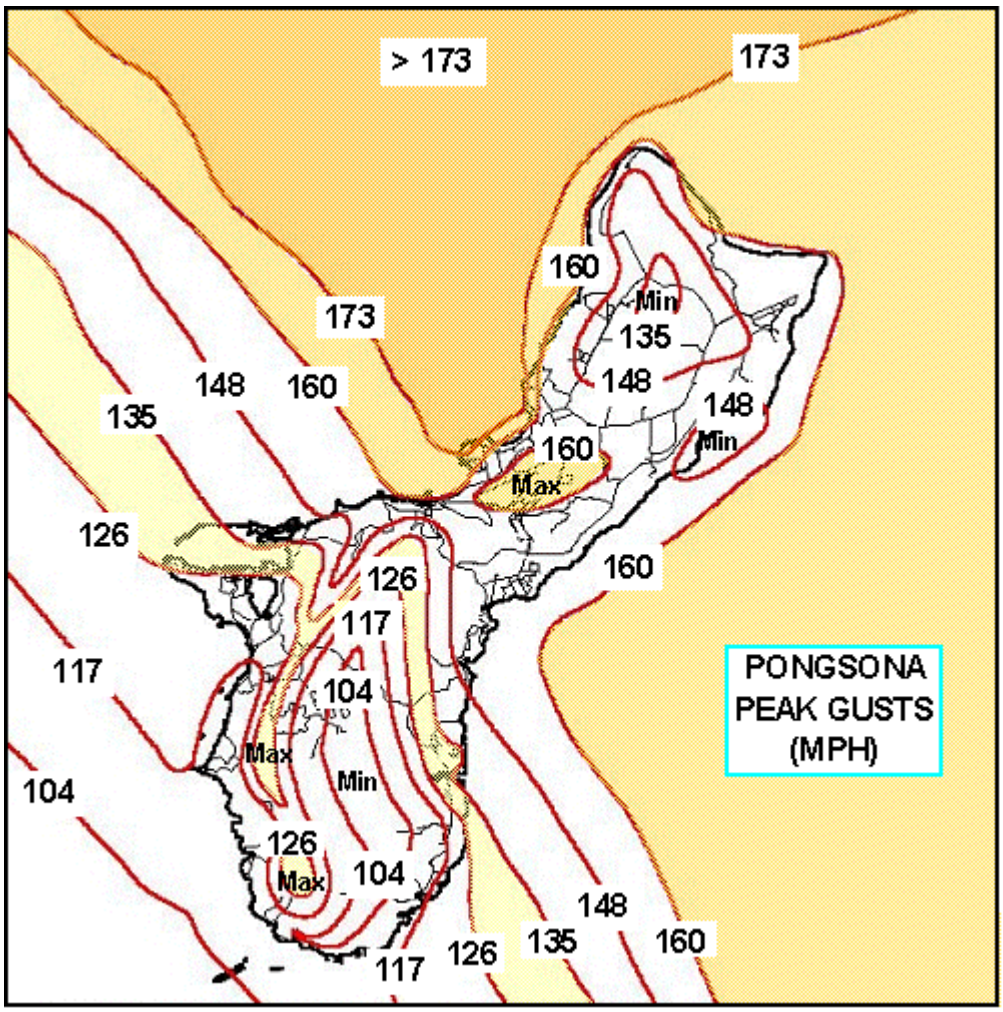

Figure 30. Analysis of peak gusts on Guam during the passage of Typhoon Pongsona on 8 December 2002. Winds are in miles per hour (MPH).

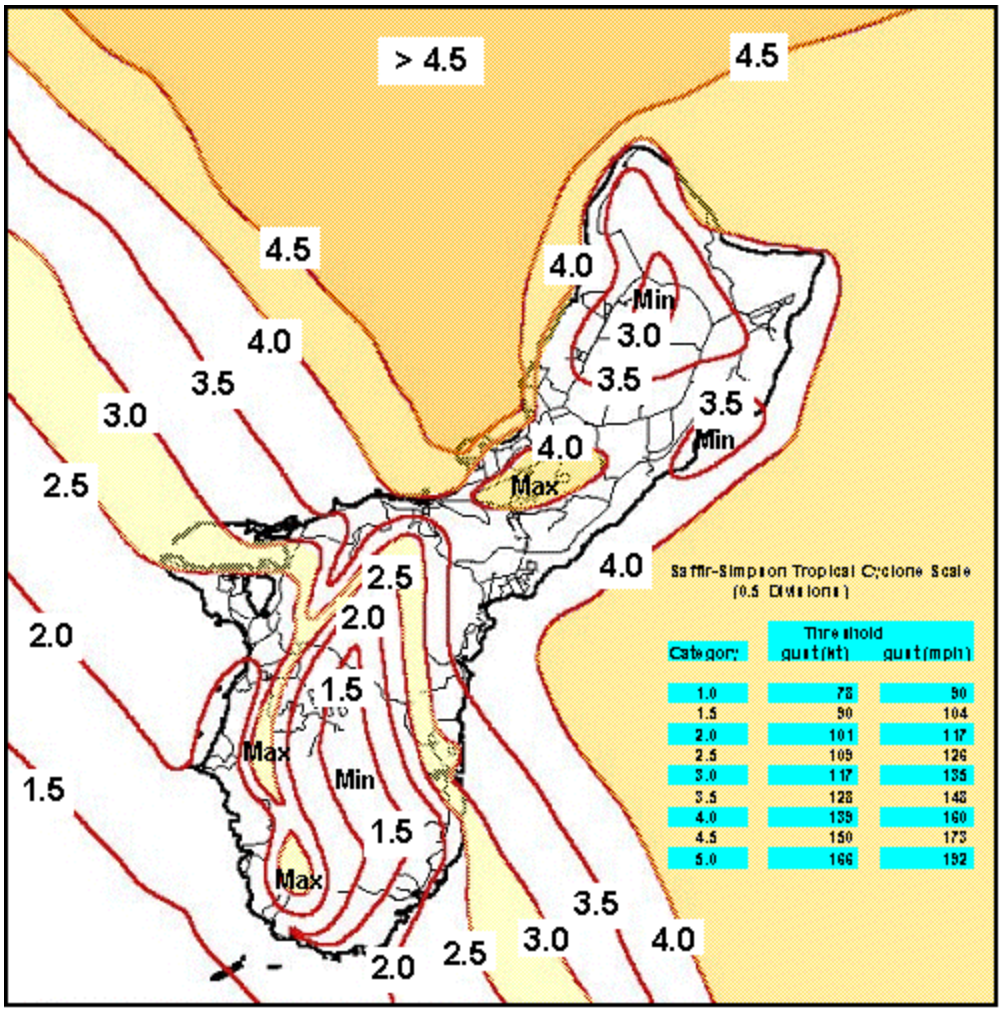

Figure 31. Pongsona peak wind distribution over Guam. Contours are in units of Saffir Simpson Tropical Cyclone Damage Scale (Guard and Lander 1999). Threshold gusts associated with each category are shown in the inset and in Appendix C.

(a) **(b)**

Figure 32. **(a)** Near coastal effects of the 22-foot storm surge observed at Songsong Village, Rota. **(b)** Effects of the surge on the fuel-loading pipeline at Songsong, Rota.

Figure 33. Destroyed wooden house and relatively unscathed reinforced concrete house in eastern Songsong Village, Rota, CNMI.

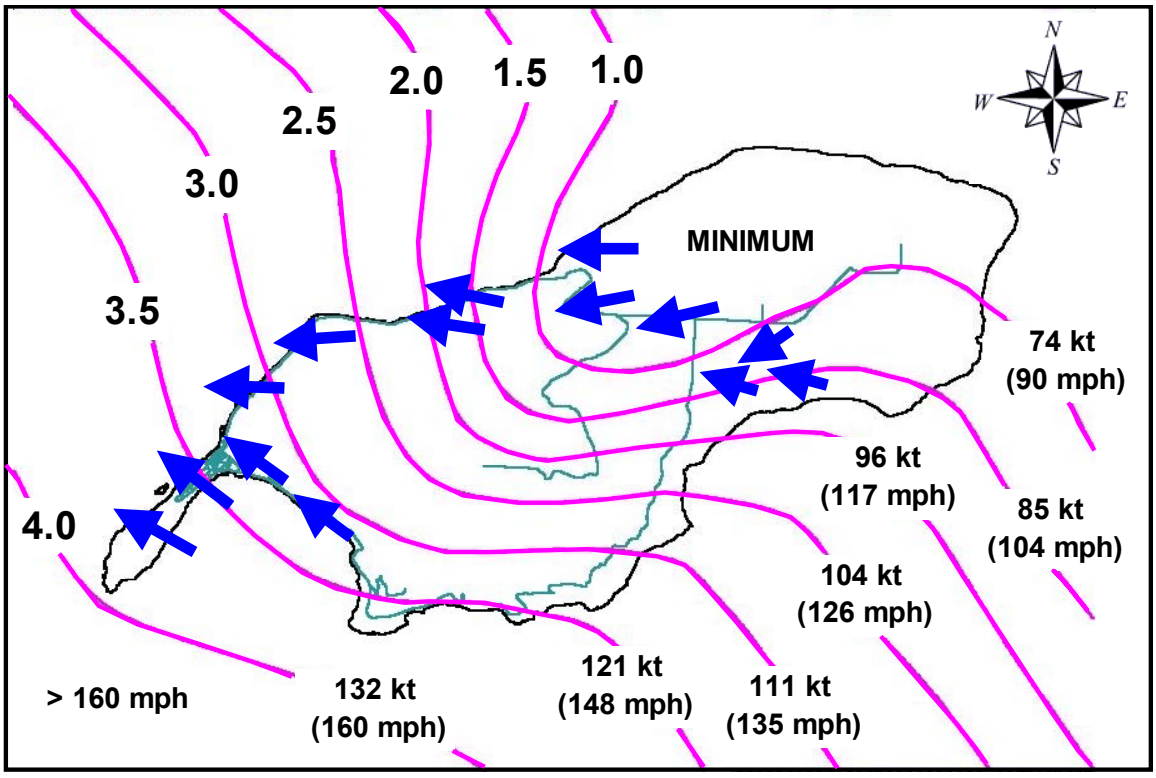

Figure 34. Analysis of peak gusts (lower numbers), damage in terms of 0.5 Saffir-Simpson Tropical Cyclone Scale Category (upper numbers), and tree fall direction (blue arrows) for Rota, CNMI during the passage of Typhoon Pongsona on 8 December 2002.